JAMES | Journal of Advances in Modeling Earth Systems

RESEARCH ARTICLE
10.1029/2019MS001971

Improving a Multilevel Turbulence Closure Model for a Shallow Lake in Comparison With Other 1-D Models

Lei Sun[1,2], Xin-Zhong Liang[2,3], Tiejun Ling[4], Min Xu[5], and Xuhui Lee[6]

[1]Climate, Environment and Sustainability Center, School of Atmosphere Science, Nanjing University of Information Science and Technology, Nanjing, China, [2]Earth System Science Interdisciplinary Center, University of Maryland, College Park, MD, USA, [3]Department of Atmospheric and Oceanic Science, University of Maryland, College Park, MD, USA, [4]Key Laboratory of Research on Marine Hazards Forecasting, National Marine Environmental Center, Beijing, China, [5]Climate Change Science Institute, Oak Ridge National Laboratory, Oak Ridge, TN, USA, [6]School of Forestry and Environmental Studies, Yale University, New Haven, CT, USA

Key Points:
- An upper ocean mixed layer model was improved for a shallow lake application with primary modifications on surface roughness, radiation extinction, and vertical mixing
- The model was intercompared against three other representative 1-D models based on different concepts in the context of using a unified surface flux scheme
- The improved model well captured the surface temperature diurnal cycle and daily to seasonal variations of Lake Taihu

Supporting Information:
- Supporting Information S1

Correspondence to:
X.-Z. Liang and T. Ling,
xliang@umd.edu;
lingtj@nmefc.cn

Citation:
Sun, L., Liang, X.-Z., Ling, T., Xu, M., & Lee, X. (2020). Improving a multilevel turbulence closure model for a shallow lake in comparison with other 1-D models. *Journal of Advances inModeling Earth Systems*, *12*, e2019MS001971. https://doi.org/10.1029/2019MS001971

Received 4 DEC 2019
Accepted 17 JUN 2020
Accepted article online 21 JUN 2020

Abstract Lakes differ from lands in water availability, heat capacity, albedo, and roughness, which affect local surface-atmospheric interactions. This study modified a multilevel upper ocean model (UOM) for lake applications and evaluated its performance in Lake Taihu (China) with comprehensive measurements against three popular one-dimensional (1-D) lake models. These models were based on different concepts, including the self-similarity (FLake), the wind-driven eddy diffusion (LISSS), the k-ε turbulence closure (SIMSTRAT), and a simplified turbulence closure (UOM). The surface flux scheme in these models was unified to exclude the discrepancies in representing air-lake exchanges. All models in their default formulations presented obvious cold water temperature biases and largely underestimated the lake surface temperature (LST) diurnal range. For each model, these deficiencies were significantly reduced by incorporating new physics schemes or calibrated tunable parameters based on systematic sensitivity tests. The primary modifications for UOM included (1) a new scheme of decreased surface roughness lengths to better characterize the shallow lake, (2) a solar radiation penetration scheme with increased light extinction coefficient and surface absorption fraction to account for the high water turbidity, and (3) turbulent Prandtl number increased by a factor of 20 to reduce the turbulent vertical mixing. All other models were improved in these three aspects (roughness, extinction, and mixing) within their original formulations. Given these improvements, UOM showed superior performance to other models in capturing LST diurnal cycle and daily to seasonal variations, as well as summer-autumn vertical stratification changes. The new UOM is well suited for application in shallow lakes.

Plain Language Summary Lakes, with unique characteristic differences from lands, play an important role on local-regional weather and climate. This study improved a multilevel upper ocean model (UOM) for a shallow lake application with primary modifications on surface roughness, radiation extinction, and vertical mixing. The model was intercompared against comprehensive measurements with three other improved one-dimensional models based on different concepts in the context of using a unified surface flux scheme to exclude the discrepancies in representing lake-air exchanges. All models in their default formulations presented obvious cold water temperature biases and largely underestimated the lake surface temperature diurnal range. Their performances were significantly improved with the proposed modifications. In particular, the improved UOM showed superior performance to other models in capturing lake surface temperature diurnal cycle and daily to seasonal variations, as well as summer-autumn vertical stratification changes. The new UOM is useful for inclusion in weather and climate models to represent shallow lake processes.

1. Introduction

Understanding land-lake-atmosphere interactions is essential to weather and climate predictions (Sharma et al., 2018). Lakes are characterized by low albedo, large heat capacity, reduced roughness, and unlimited water supply when compared to the surrounding land surfaces. These differences affect local surface-atmospheric exchanges of energy, moisture, and momentum fluxes, depending strongly on lake size, depth and location, and seasons. These local effects impact weather and climate at regional scales through surface-atmospheric interactions (Bennington et al., 2014; Bonan, 1995; Diallo et al., 2018; Dutra et al., 2010;

Long et al., 2007; Notaro et al., 2013; Samuelsson et al., 2010; Thiery et al., 2015). As numerical weather or climate prediction model resolution continuously increases, correctly resolving air-lake interactions becomes indispensable.

A number of lake models have been developed, ranging from simple one-dimensional (1-D) bulk model to complex three-dimensional (3-D) hydrodynamic models and tested for their performances on various lakes with different characteristics. Compared to 1-D models that neglect the in-lake horizontal processes, 3-D models show advantages in reproducing the thermal structure, especially in large, deep lakes, such as the North American Great Lakes (Bai et al., 2013; Dupont et al., 2012; Xue et al., 2017). However, for computational efficiency, coupling simplicity, and the fact that horizontal gradients are negligible in small or medium-sized lakes, 1-D models gain much popularity and have been widely incorporated into weather models (Gu et al., 2015), regional climate models (Bennington et al., 2014; Liang et al., 2012), and general circulation models (Donner et al., 2011; Subin et al., 2012). This study focuses on 1-D lake models.

The current 1-D lake models fall into three primary categories (Hostetler & Bartlein, 1990; Joehnk & Umlauf, 2001; MacKay, 2012). These include (1) one-layer bulk models (Goyette et al., 2000; Strong et al., 2014) that assume a completely mixed slab, (2) two-layer integral model (e.g., FLake, Mironov et al., 2010) that consists of an upper mixed layer and lower thermocline formed based on the self-similarity concept, and (3) multilayer models based on wind-driven eddy diffusion parameterization (Hostetler et al., 1993; Subin et al., 2012) or turbulence closures (Gaudard et al., 2017; Goudsmit et al., 2002; Stepanenko et al., 2016). A series of comparison studies have been conducted to evaluate performance differences among available models simulating lake surface temperature (LST), mixing regimes and ice cover duration as well as surface turbulent heat fluxes (Haddout et al., 2018; Martynov et al., 2010; Perroud et al., 2009; Yao et al., 2014). In particular, the Lake Model Intercomparison Project (LakeMIP) was initiated in 2008 (Stepanenko et al., 2010) and have compared diverse 1-D lake models for applications in several representative lakes, varying from a boreal, small, shallow Lake Valkea-Kotinen (Stepanenko et al., 2014) to a tropical, large, deep Lake Kivu (Thiery et al., 2014). Advantages and disadvantages are both obvious for all models, and no single model is the best for all applications because of different lake characteristics and model physics representations.

Two-equation turbulence closure schemes have been demonstrated to perform well in reproducing the vertical structure of turbulence and widely applied in lake or ocean mixed layer models for both effectiveness and efficiency (Burchard, 2002; Burchard et al., 1998; Chen et al., 2003; Goudsmit et al., 2002; Mellor & Yamada, 1982; Stepanenko et al., 2016). A simplified one-equation turbulence closure, which predicts explicitly only the turbulence kinetic energy (TKE) while diagnosing the turbulence length scale or dissipation of TKE, has also been used effectively in lake and ocean modeling studies (Axell & Liungman, 2001; Herb & Stefan, 2005). Based on the one-equation TKE closure scheme (Noh, 1996; Noh & Jin Kim, 1999; Noh et al., 2011), Ling et al. (2015) developed a comprehensive multilevel upper ocean model (UOM) to realistically reproduce the diurnal cycle and daily variability of sea surface temperature (SST) when driven by observed surface conditions. The UOM has been fully coupled with the state-of-the-art regional Climate-Weather Research and Forecasting model (CWRF) to resolve transient air-sea interactions for long-term climate simulations (Liang et al., 2012, 2018). The main purpose of this study is to further improve the UOM for freshwater lake applications and compare its performance with three representative 1-D models. These models are based on different concepts, using the self-similarity assumption in the Freshwater Lake model (FLake; Mironov et al., 2010), the wind-driven eddy diffusion parameterization in the Lake, Ice, Snow and Sediment Simulator (LISSS; Gu et al., 2015; Subin et al., 2012), and the k-ε turbulence closure in SIMSTRAT (Goudsmit et al., 2002). Together, they represent a wide range of model complexities.

Accurate representation of lake surface flux exchanges with the atmosphere is essential for models to reproduce LST variations and mixing regimes. Previous intercomparison studies, however, have generally evaluated lake models' performance based on their built-in surface flux schemes, obviously due to technical difficulties from different code structures. In this study, the structure of all models in comparison was reengineered using a standard interface for initialization and integration and thus kept the surface driver of the flux calculation consistent among the models. The extended surface scheme (Oleson et al., 2013; Zeng et al., 1998) used in both UOM and LISSS was implemented for FLake and SIMSTRAT. Unifying the

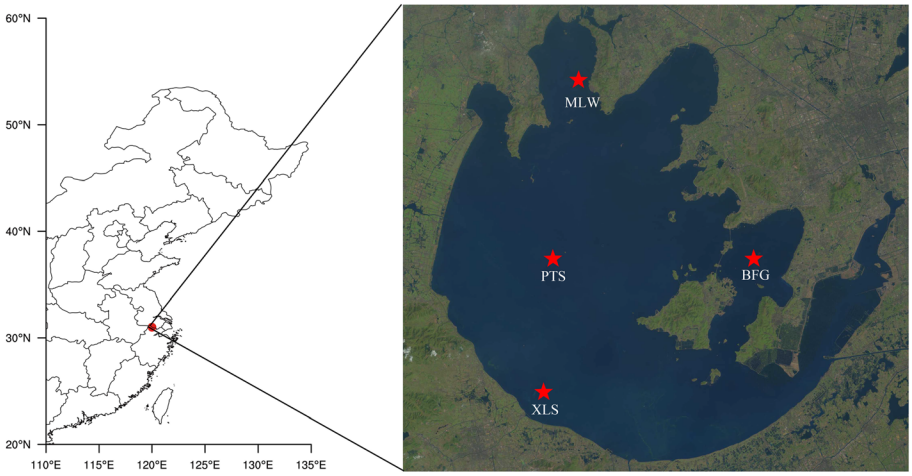

Figure 1. Geographical location and Landsat 8 image of the Lake Taihu with red stars denoting the locations of covariance mesonet at measurement sites.

surface flux calculation as such eliminated the source of discrepancies caused by varying lake-atmospheric exchanges among participating models.

Lakes are characterized by varying properties so that numerical models typically require fine-tuning to achieve best performance. This study first refined the responsive physics schemes and key parameters pertaining to each model's original formulation through a systematic sensitivity analysis to improve the overall performance and then compared these improved models for skills in capturing observed characteristics. Section 2 describes Lake Taihu (China) as the study site with comprehensive measurements. Section 3 presents a brief overview of each model's existing formulation and proposed key improvements, especially to UOM. Section 4 focuses on sensitivity analyses and refinements to individual models. Section 5 compares the improved models' performance in capturing observed characteristics. Section 6 summarizes the conclusion.

2. Lake Taihu—The Study Site and Measurements

Lake Taihu, located in the southeastern China (Yangtze River Delta, Figure 1), has a large surface area of 2,400 km^2 and a mean depth of 1.9 m. It is chosen as our study site for three main reasons. First, it is a very shallow lake and typically polymictic, experiencing strong diurnal turnover, so that it is a good target for assessing models' abilities in representing the LST diurnal cycle and seasonal variations. Second, improving LST prediction has an enormous benefit and water temperatures critically determine the population density of cyanobacteria (blue-green algae), which have long been regarded as a cause of taste and odor problems in drinking water from Lake Taihu (Persson, 1983; Xu et al., 2008). Third, modeling studies on subtropical, shallow lakes have been very limited due to data lack, while the high-quality measurements provided from the Taihu eddy flux network (Lee et al., 2014) offer a unique opportunity to test, improve, and compare models. Deng et al. (2013) tuned LISSS based on these observations but only focused on surface temperature regardless of the lake thermal structure. This study provides a comprehensive intercomparison of 1-D lake models.

An advanced eddy covariance network around Lake Taihu, consisting of five lake sites and one land site, was constructed in 2010 and has since been monitoring the air-lake interactions (Lee et al., 2014). The measurement consists of meteorological fields (wind speed and direction, air temperature, pressure, and humidity), turbulent heat fluxes, radiation fluxes, and water temperatures at 20, 50, 100, and 150 cm depth as well as underlying sediment surface temperature. Observations from four measurement sites (Figure 1), including Meiliangwan (MLW), Bifenggang (BFG), Xiaoleishan (XLS), and Pingtaishan (PTS) sites, across the lake are used in this study. In particular, the modeling study focused on MLW site because of its enhanced high-quality observations and absence of submersed macrophytes, which eliminates their influence on turbulence mixing (Herb & Stefan, 2005).

3. Model Formulations and Proposed Improvements

3.1. Existing Lake Model Formulations

The UOM is based on a system of prognostic equations of horizontal currents, potential temperature, salinity, and TKE, which were first proposed by Noh and Fernando (1991) with subsequent improvements (Noh, 1996; Noh & Jin Kim, 1999; Noh et al., 2011). Ling et al. (2015) reengineered and significantly improved the model in resolving SST diurnal cycle by incorporating a momentum penetration scheme (Zhang & Zebiak, 2002), a two-band shortwave radiation penetration scheme (Kara et al., 2005), a cool-skin temperature scheme (Zeng & Beljaars, 2005), a vertical grid stretch scheme (Mcwilliams et al., 1990), and a semi-implicit time integration scheme with a SST nudging algorithm. The UOM incorporates a one-equation TKE closure scheme, in which the TKE per unit mass k (J kg^{-1}) is predicted dynamically with a diagnostic turbulence length scale l (m) as defined in section 3.2. Here l is divided by $(1+c_1R_t)^{1/2}$ to consider the stratification effect (Noh, 1996). In particular, $c_1 = 0.3$ is a dimensionless empirical number and $R_t = \frac{N^2l^2}{2k}$ is the Richardson number for turbulence eddies, where N is the buoyancy frequency (s^{-1}). The eddy diffusivities for momentum ν_m (m^2 s^{-1}) and heat ν_h (m^2 s^{-1}) are determined by $c_k\sqrt{2k}l$ and $\frac{\nu_m}{Pr_t}$, respectively, where $c_k = 0.39$ is a dimensionless empirical constant and Pr_t is the turbulent Prandtl number.

The SIMSTRAT was updated by Goudsmit et al. (2002) from the buoyancy-extended k-ε turbulence model developed by Burchard et al. (1998). Two prognostic equations are solved to predict the dynamics of the TKE per unit mass k (J kg^{-1}) and the TKE dissipation rate ε (W kg^{-1}). The TKE is generated from the shear stress and consumed by the dissipation. The buoyancy flux acts as a source (sink) of TKE in the case of unstable mixing (stable stratification). The eddy viscosity is given as $\nu_m = c_\mu\frac{k^2}{\varepsilon}$(m^2 s^{-1}) and the eddy diffusivity as $\nu_h = c_\mu^{'}\frac{k^2}{\varepsilon}$(m^2 s$^{-1)}$. In the standard k-ε model, $c_\mu = 0.09$ is a dimensionless empirical constant and $c_\mu^{'}=\frac{c_\mu}{Pr_t}$. Alternatively, c_μ and $c_\mu^{'}$ can also be calculated using the stability function proposed by Galperin et al. (1988) to account for the stratification effect.

The LISSS was developed by Subin et al. (2012) from Hostetler et al. (1993) with several major improvements, including an advanced parameterization of surface properties, a comprehensive treatment of snow and ice physics, and incorporation of an underlying sediment thermal submodel. The LST is solved in a surface energy balance equation using the Newton-Raphson method, while lake temperatures in each internal layer and at sediment are solved by the thermal diffusion equation using the semi-implicit Crank-Nicholson method. The eddy diffusivity is given by $\nu_h = m_d\left(\nu_e + \nu_h^{'}\right)$(m^2 s^{-1}), where $m_d = \begin{cases} 1, & D<25\text{ m} \\ 10, & D \geq 25\text{ m} \end{cases}$ is the mixing factor depending on the lake depth. The wind-driven eddy diffusion in the unfrozen lake for layer i is parameterized by $\nu_e = \frac{1.2\times10^{-3}u_2\kappa z_i\exp\left(-k^*z_i\right)}{Pr_t^0\left\{1+37\left[-\frac{1}{20}+\frac{1}{20}\sqrt{1+40\left(\frac{N\kappa z_i}{1.2\times10^{-3}u_2\exp\left(-k^*z_i\right)}\right)^2}\right]^2\right\}}$(m^2 s^{-1}), where u_2 is the wind speed (m s^{-1}) at 2 m, $\kappa = 0.4$ is the von Karman constant, z_i is the node depth (m) located in the center of each layer (Table 1), $Pr_t^0 = 1$ is the neutral value of the turbulent Prandtl number, N is the buoyancy frequency (s^{-1}), and $\nu_h^{'} = 1.5\times10^{-7}$ m^2 s^{-1} is the molecular diffusivity. In particular, k^*=$6.6u_2^{-1.84}\sqrt{|\sin\phi|}$, where ϕ is the latitude and is the Ekman profile parameter estimated from the best fit of observations (Henderson-Sellers, 1985; Hostetler & Bartlein, 1990).

The FLake is a two-layer bulk model, consisting of an upper mixed layer and a lower thermocline down to the lake bottom, based on the assumption of self-similarity in the thermocline structure (Mironov et al., 2010). The temperature profile in the thermocline is described by a fourth-order polynomial function of shape factor. The snow/ice cover as well as underlying sediment layer is also included and based on the similar parametric concept.

Table 1
Control and Sensitivity Experiments for 1-D Lake Models

Models	Period/Time step (s)	Grid spacing (m)/no. of layers	Surface scheme	Model parameters	Control	Exp1	Exp2	Exp3	Exp4
UOM	2012.07.20 to 2012.09.30/120	0.1/20	Zeng et al., 1998	Surface roughness (m)	0.001	Subin et al. (2012)	Subin et al. (2012)	Subin et al. (2012)	
				Extinction coefficient (m^{-1})	Kara et al. (2005)	Kara et a1. (2005)	3	3	
				Absorption fraction	0	0	0.8	0.8	
				Turbulent Prandtl number	1	1	1	20	
SIMSTRAT				Surface roughness (m)	0.001	Subin et al. (2012)	Subin et al. (2012)	Subin et al. (2012)	
				Extinction coefficient (m^{-1})	0.89	0.89	3	3	
				Absorption fraction	0.4	0.4	0.8	0.8	
				Turbulent Prandtl number	1	1	1	20	
LISSS				Surface roughness (m)	0.001	Subin et al. (2012)	Subin et al. (2012)	Subin et al. (2012)	Subin et al. (2012)
				Extinction coefficient (m^{-1})	0.89	0.89	3	3	3
				Mixing factor	1	1	1	0.01	0.01
				Soil layer	T	T	T	T	F
FLake		-/2		Surface roughness (m)	0.001	Subin et al. (2012)	Subin et al. (2012)		Subin et al. (2012)
				Extinction coefficient (m^{-1})	0.89	0.89	3		3
				Soil layer	T	T	T		F

Note. Dates are formatted as YYYY.MM.DD.

3.2. Proposed UOM Improvements

Several modifications have been made to UOM for its freshwater lake application in this study. First, the turbulence length scale l (m) is originally diagnosed using the well-known Blackadar formula $l = l_g\, l_0/(l_g + l_0)$, where $l_g = \kappa(z + z_0)$ is the geometric length scale (m), l_0 the mixed layer depth (m) determined by the depth of maximum buoyancy gradient (Noh & Jin Kim, 1999), z_0 the surface roughness length (m), and $\kappa = 0.4$ the von Karman constant. This formula has often been used in the atmospheric boundary layer and in the ocean mixed layer (Klein & Coantic, 1981; Noh, 1996) to describe the wall effect of the air-sea interface on l. For a shallow lake, however, the bottom boundary effect also tends to limit the sizes of turbulent eddies. Therefore, in the case of two-boundaries, we follow Axell and Liungman (2001):

$$\frac{1}{l_g^2} = \frac{1}{\kappa^2 (z + z_0)^2} + \frac{1}{\kappa^2 (D + z + z_0)^2}, \tag{1}$$

where D is the lake depth and set to 2 m for Lake Taihu.

Second, the freshwater density ρ (kg m^{-3}) is approximated as a function of water temperature (Hostetler & Bartlein, 1990) instead of the background sea water density used in ocean application:

$$\rho = 1,000\left(1 - 1.9549 \times 10^{-5} |T - T_{md}|^{1.68}\right), \tag{2}$$

where T is the water temperature in degrees Celsius and $T_{md} = 3.85$°C is the temperature of maximum water density. In addition, the freshwater specific heat capacity $C_p$is fixed as 4.188×10^3 J kg^{-1} K^{-1}.

Third, Ling et al. (2015) introduced a two-band solar penetration scheme (Kara et al., 2005) to improve the radiation distribution in the oceanic mixed layer. In unfrozen lakes, a fraction β of the near-infrared shortwave radiation is absorbed within the top layer of a few centimeters, while the visible radiation penetrates into the water at depth z (m) by a factor according to the extinction law:

$$Q(z) = Q_0(1-\beta)\exp(-\eta z), \tag{3}$$

where Q_0 is the net total solar radiation (W m^{-2}) at lake surface and η (m^{-1}) is the light extinction coefficient depending on water turbidity among other factors. In this study, Q_0 takes directly the net shortwave radiation as measured and simulated in the model, both of which has already accounted for the effect of surface albedo.

Fourth, surface roughness lengths are the key parameters for the drag coefficients, which in turn determine the fluxes of momentum, sensible, and latent heat. The original UOM uses the same parameterization of the roughness length z_0 (m) in all cases. A new scheme (Subin et al., 2012; Zilitinkevich et al., 2001) is now adopted to parameterize the roughness length differently for momentum (z_{0m}), heat (z_{0h}), and vapor (z_{0q}) as follows:

$$z_{0m} = max\left(\frac{\alpha\upsilon}{u_*}, \frac{cu_*^2}{g}\right), \tag{4}$$

where α is a dimensionless constant set to 0.01, u_* and υ the water surface friction velocity (m s^{-1}) and air kinematic viscosity (m^2 s^{-1}), respectively. The g (m s^{-2}) is the acceleration of gravity, and c is the dimensionless effective Charnock coefficient under the limitation of lake fetch and depth:

$$c = c_{min} + (c_{max} - c_{min})\exp\left(-min\left(f_c{}^{-1}\left(\frac{Fg}{u_*^2}\right)^{1/3}, \zeta\frac{\sqrt{Dg}}{u_*}\right)\right), \tag{5}$$

where c_{min}, c_{max}, f_c, and ? are dimensionless empirical constants and set to 0.01, 0.11, 22, and 1, respectively, following Subin et al. (2012). $F = 25D$ is the lake fetch (m) depending on the lake depth D. Although Lake Taihu probably has the largest fetch among shallow lakes (Deng et al., 2013), sensitivity of roughness length to fetch was found to be very small (Subin et al., 2012). Roughness lengths for heat and water vapor are calculated from

$$z_{0h} = z_{0m}\exp\left(-\frac{\kappa}{P_r}\left(4\sqrt{R_0} - 3.2\right)\right), \tag{6}$$

$$z_{0q} = z_{0m}\exp\left(-\frac{\kappa}{S_c}\left(4\sqrt{R_0} - 3.2\right)\right), \tag{7}$$

where $P_r = 0.71$ is the air molecular Prandtl number and $S_c = 0.66$ is the molecular Schmidt number for water in air.

$$R_0 = max\left(\frac{z_{0m}u_*}{\upsilon}, 0.1\right). \tag{8}$$

Finally, the molecular diffusion effects, absent in the origin UOM, are now added to the governing transport equations by including the terms of the molecular viscosity $\nu_m^{'}$=1.5×10^{-6} m^2 s^{-1} and diffusivity $\nu_h^{'}$=1.5×10^{-7} m^2 s^{-1}. Since Lake Taihu remains ice-free year around, the ice and snow processes are not treated in this study. As discussed below, most of the above modifications have been incorporated to improve the other three lake models.

4. Model Localization

4.1. Control Experiment

Each model was first tuned by improving sensitive formulations and tuning related parameters for more realistic performance in Lake Taihu. In the control experiment, surface roughness lengths were set to a constant

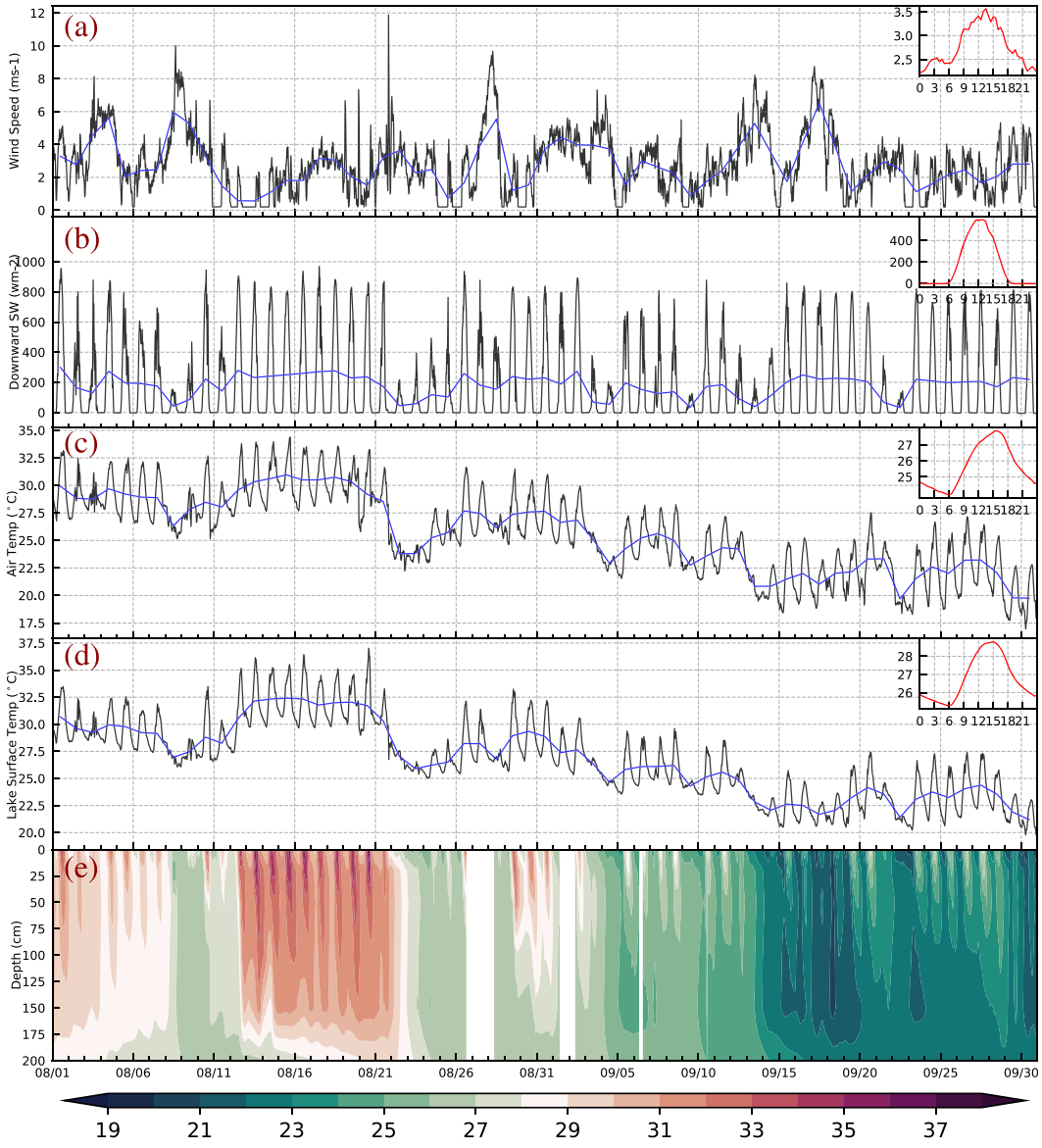

Figure 2. Measurements of time series of (a) wind speed, (b) downward shortwave flux, (c) air temperature, (d) lake surface temperature deduced from longwave flux using Stefan-Boltzmann law, and (e) water temperatures at MLW site from 1 August to 30 September in 2012 with the blue line and inset denoting daily mean values and averaged diurnal cycle, respectively.

0.001 m for all models following Weather Research and Forecasting (WRF) model-lake applications (Gu et al., 2015; Huang et al., 2019; Xu et al., 2016). Surface solar absorption fraction β was set to 0.4 with the extinction coefficient as $\eta = 1.1925D^{-0.424} \approx 0.89$ for $D = 2$ m (Hakanson, 1995), except for UOM, which uses its default two-band scheme (Kara et al., 2005). For the heat exchange with underlying sediments, a no-flux condition was used for two turbulence models and the sediment thermal schemes were activated in LISSS and FLake. The default mixing factor m_d in LISSS and turbulent Prandtl number Pr_t (ratio of momentum diffusivity to thermal diffusivity) in turbulent models were both set to 1. In UOM, the cool-skin and warm-layer, surface momentum flux penetration, SST nudging, and other specific schemes that were designed for ocean mixed layers were deactivated in Lake Taihu. In SIMSTRAT, the morphometry and internal seiche effects were eliminated and the geothermal heat flux was set to 0 W m^{-2}. Moreover, the standard k-ε model is used in SIMSTRAT. Similarly, the stratification effect on turbulence length scale was deactivated in UOM.

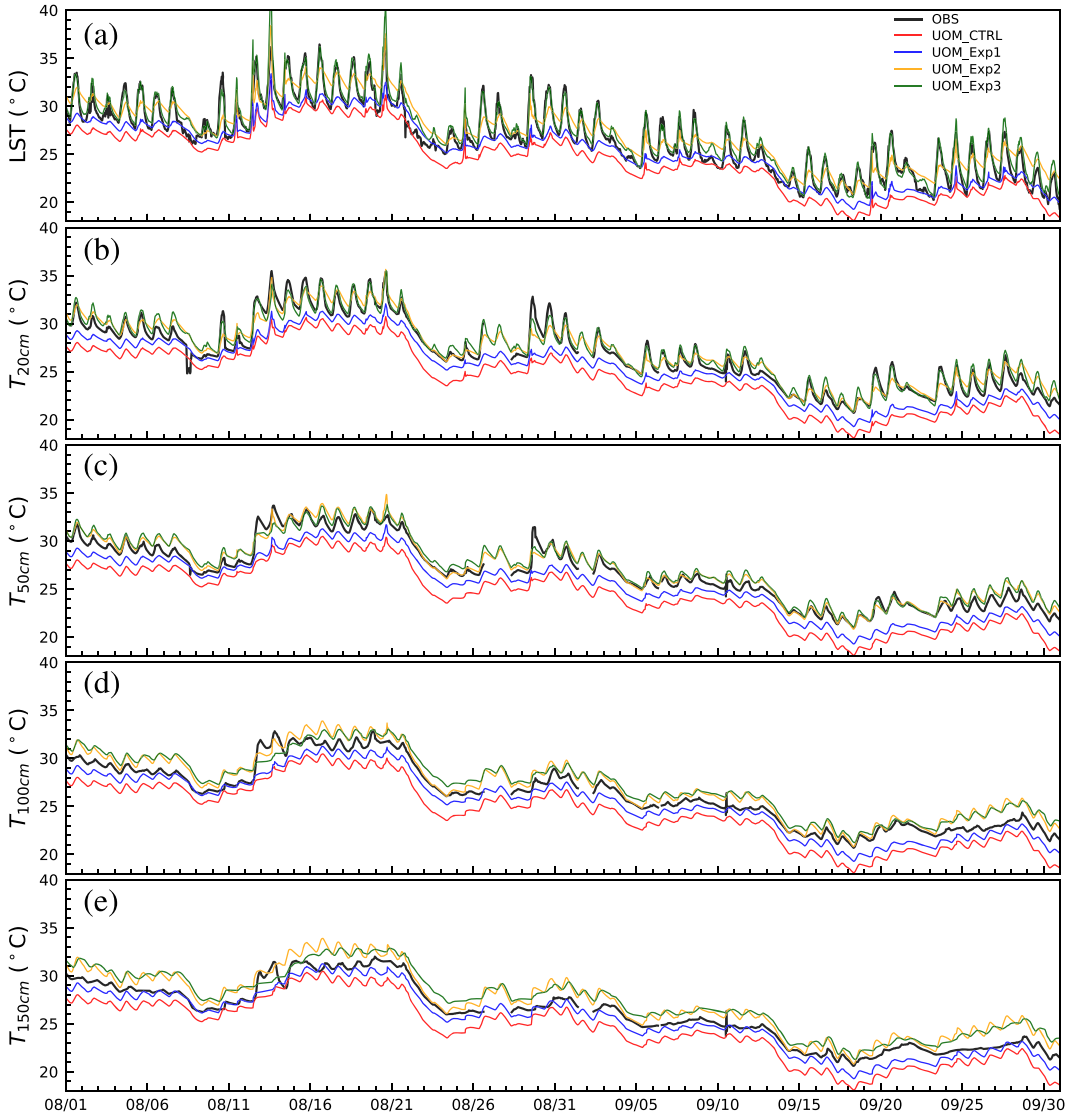

Figure 3. Half-hourly series of temperature observed (black) and simulated by UOM control and sensitivity experiments at (a) lake surface, and the depths of (b) 20, (c) 50, (d) 100, and (e) 150 cm.

Other than the above, all configurations, including vertical discretization (except for FLake), integration time steps, and initial conditions, were kept identical to the extent possible for all models (Table 1). Results from additional tests show that the integration time step within the range of 60–180 s has almost no effect on the model performance, while the vertical grid spacing between 0.05 and 0.2 m has minor effects on representing the lake thermal structure in UOM and other models. The control simulation was integrated from 20 July to 30 September 2012. This period was chosen because it was a transition period containing both summer warming and autumn cooling (Figure 2). The initial 10 days was considered the spin-up time, which was sufficient for Lake Taihu due to its shallowness, and thus discarded in the analysis.

In Lake Taihu, LST is mainly regulated by surface air temperature (Figures 2c and 2d) as a result of its shallowness and displays an obvious diurnal cycle with an amplitude of about 3.5°C. Figures 3–6 compare the UOM, SIMSTRAT, LISSS, and FLake simulated half-hourly series of LST and water temperatures at each probing depth, while Figure 7 summarizes their overall performance in temporal correlations (corr) and root-mean-square errors (rmse) against observations using the Taylor (2001) diagram. All control model simulations underestimated LST by 1.2–2.3°C and its diurnal range by 2.4–2.8°C (Figures 8a–8d) despite generally capturing its seasonal variation with the corr around 0.9. This cold bias could be ascribed to

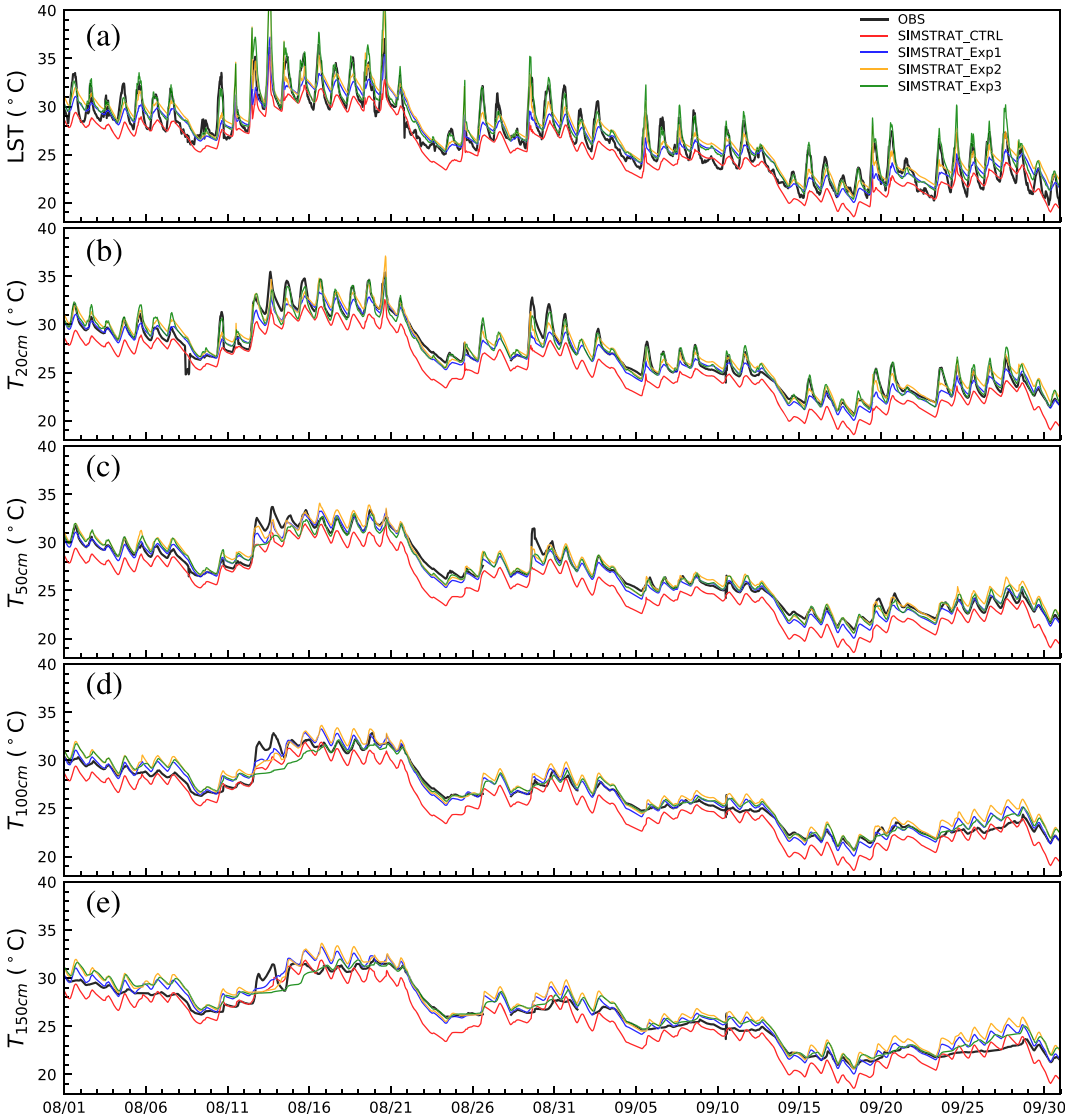

Figure 4. Same as Figure 3 except for SIMSTRAT.

excessive surface heat flux loss, insufficient shortwave radiation absorption, and overestimated vertical heat diffusivity (as revealed by the nearly uniform vertical water temperature profile). In the cloudy and windy days such as 8 August 2012 (Figure 2), less solar radiation together with stronger wind ventilation cooled the water column more and resulted in more complete mixing. On the other hand, the lake exhibited stronger stratification in the sunny and calm days such as in the mid-August. In spite of these biases, all 1-D models could generally reproduce the lake's response to changes of weather conditions. Notably, they all did well at capturing the two obvious frontal events around 23 August and 12 September 2012 that caused rapid LST cooling.

4.2. Sensitivity Experiments

For Lake Taihu, Huang et al. (2009) suggested light extinction parameters η of 4–8 m^{-1} and β of 0.55–0.8 according to observations at MLW site. Gu et al. (2013) and Deng et al. (2013) indicated that the LISSS performance was sensitive to several parameters including surface roughness lengths and solar radiation extinction parameters. Thus, a set of sensitivity experiments (summarized in Table 1) were conducted by *incrementally* adjusting key parameters of existing formulations or employing new physics schemes to improve the skill of each individual model based on previous studies and our offline tests

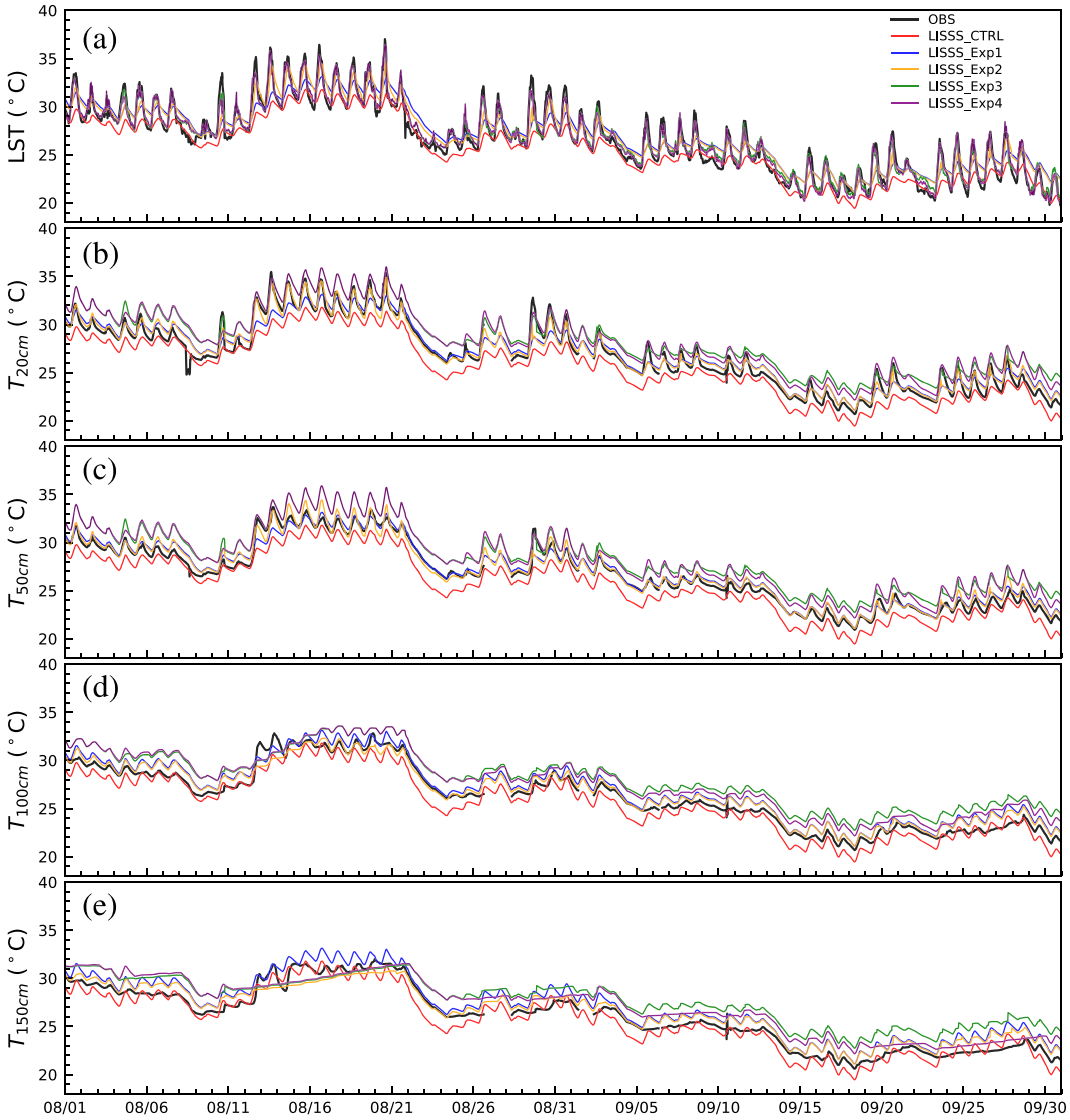

Figure 5. Same as Figure 3 except for LISSS.

(Deng et al., 2013; Gu et al., 2013; Huang et al., 2009, 2019; Ling et al., 2015; Schmid & Köster, 2016). Additional experiments were conducted using LISSS and FLake by deactivating the underlying sediment submodel to clarify the role of sediments on the lake thermal regime. For this the sediment scheme was explicitly switched off in FLake and the no-flux bottom condition was used in LISSS. The subsections below describe the results from these sensitivity experiments.

4.2.1. Surface Roughness

In reality, z_{0m} may vary with the magnitude of friction velocity and $z_{0h,q}$ can be considerably smaller than z_{0m} because heat and water vapor are transported by the interfacial sublayer molecular diffusion while momentum is transferred by the pressure forces acting on roughness elements (Charusombat et al., 2018; Kantha & Clayson, 2000). Xu et al. (2016) and Huang et al. (2019) replaced these prescribed constants with parameterized surface roughness lengths (Subin et al., 2012; Zilitinkevich et al., 2001) in Lake Erhai and Lake Nam Co (in highlands at southeastern and central Tibetan Plateau) to diminish the upward latent and sensible heat fluxes, which significantly reduced the LST cold bias.

In Exp1, we used the parameterized roughness lengths (Equations 4–8). The roughness length scales for temperature and humidity, varying from 10^{-5} to 10^{-6} m, were much smaller than the original constants

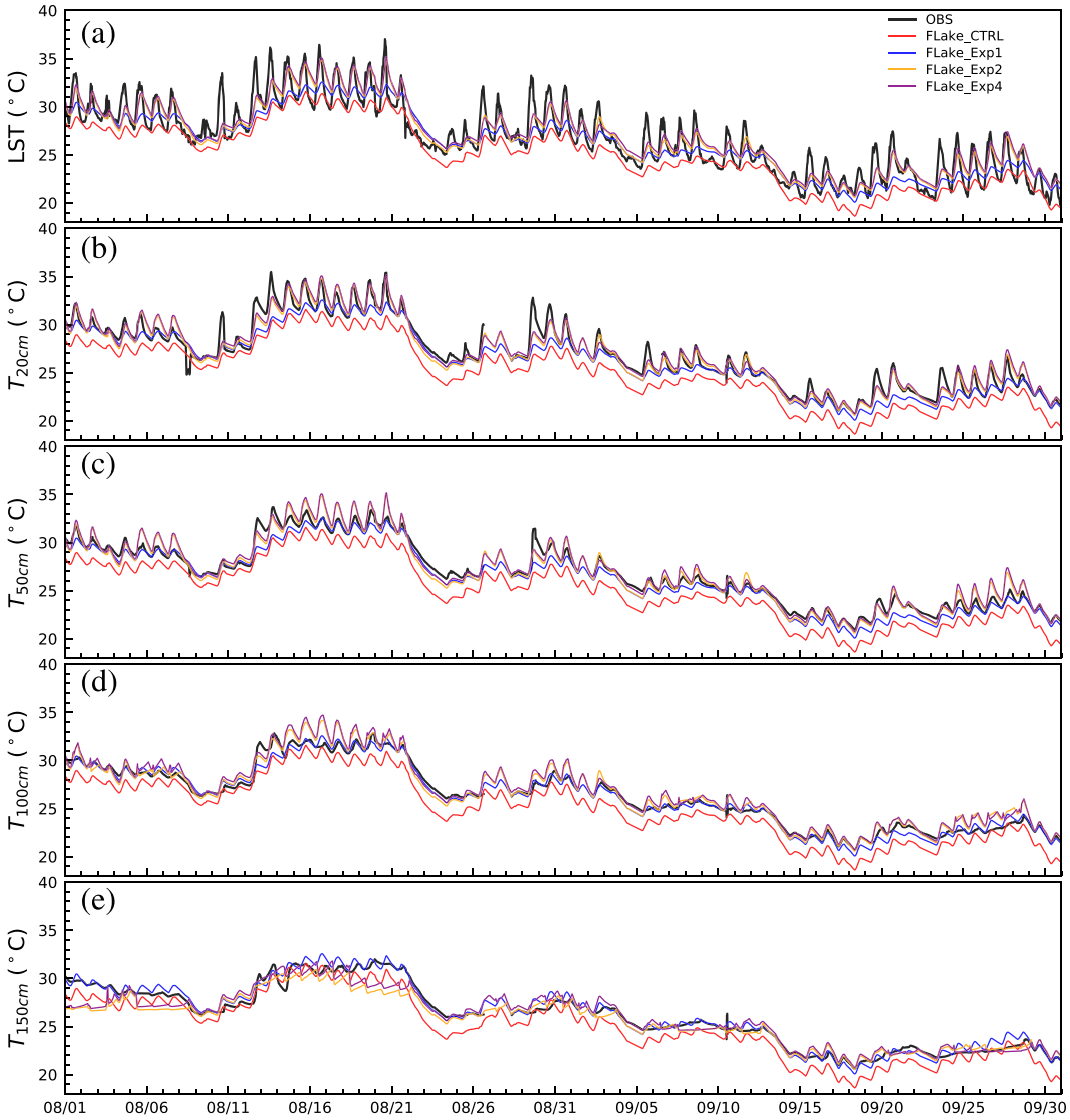

Figure 6. Same as Figure 3 except for FLake.

prescribed and thus substantially diminish the overpredicted turbulent heat fluxes compared to the control experiment. In UOM, the LST cold bias was reduced from 2.3°C to 1.3°C on average (Figure 3a) and also rmse from 2.73°C to 1.99°C (Figure 7), with little change in the diurnal range (Figure 8a). The cold bias reduction was systematic in water temperatures as in LST. All other lake models behaved very similarly when adopting the same parameterization.

4.2.2. Solar Penetration

In Exp2, on the top of surface roughness change in Exp1, we used the simple solar penetration formula (Equation 3) with the extinction coefficient η set to 3 m^{-1} instead of the default scheme of Kara et al. (2005). The absorption coefficient β was set to 0.8 following Gu et al. (2013) to depict the poor water quality of Lake Taihu resulting from heavy pollutants and frequent algal outbreaks. By the default scheme, only 13.5% and 77.4% of the net shortwave radiation were absorbed in the surface layer (0.1 m) and the entire column (2 m). The radiation unabsorbed in the upper layers would be used to heat bottom sediment layers in LISSS and FLake but ignored in UOM and SIMSTRAT without underlying layers, thus causing cold biases in the total water column. The new formula increased the absorption to 85.2% and 99.9%, respectively. As a result of absorbing more solar radiation in the surface layer, the LST cold bias in UOM was further reduced by roughly 1.7°C (Figure 3a), leading to a higher Taylor skill score (Figure 7). The whole water column was

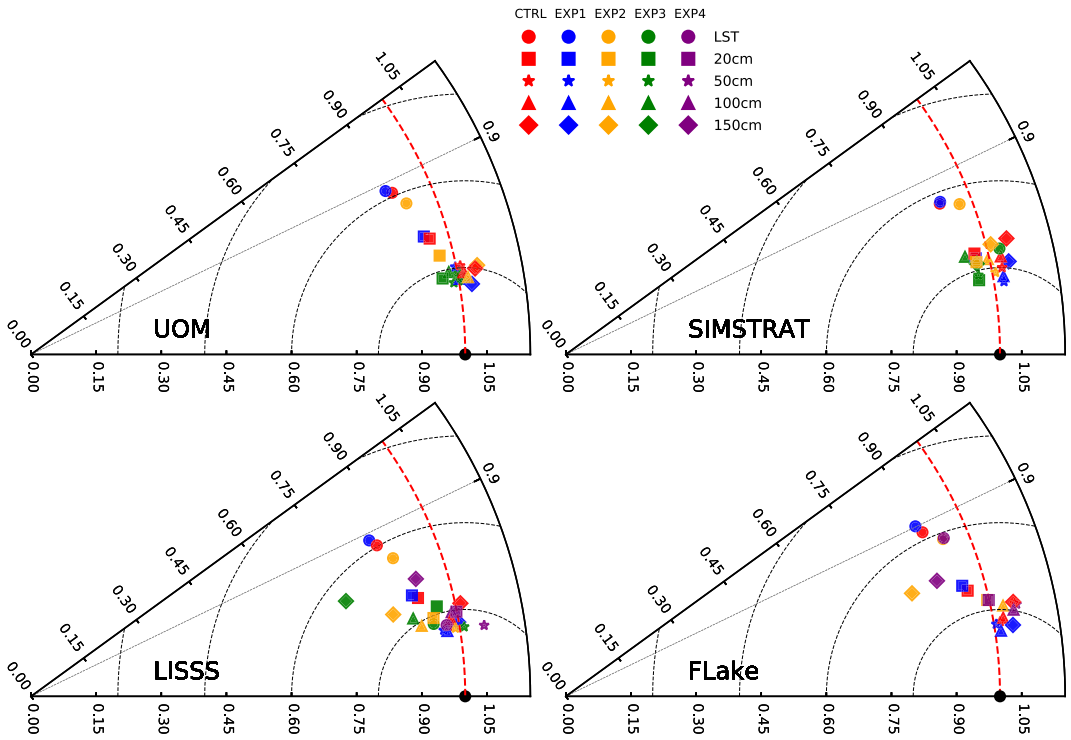

Figure 7. Taylor diagram of pattern statistics comparing control and sensitivity experiments overall performance in simulating lake surface temperature and water temperatures (20, 50, 100, and 150 cm) for each 1-D lake model.

also warmed by 1.8°C (Figure 3). However, the LST diurnal range underestimation still remained (Figure 8a). All other lake models responded very similarly to this change in solar penetration (Figures 4–6).

4.2.3. Turbulent Mixing

Lake Taihu commonly experiences strong daytime stratification especially in summer season (Figure 2e) due to its extreme shallowness. However, the water column still presents nearly uniform vertical temperature profile in both model simulations (Figures S1 and S2 in the supporting information), which indicates the substantial overestimation of vertical mixing and results in the extremely underestimated LST diurnal cycle.

The design of a 1-D lake model is based on the assumption that the effect of horizontal gradients is negligible. The missing horizontal processes, compared to 3-D hydrodynamic models such as FVCOM (Chen et al., 2003), generally play an important role only in simulations of large and deep lakes such as Lake Superior (Bai et al., 2013; Xue et al., 2017). Especially, horizontal advection can be neglected with almost no effect in Lake Taihu, in which little spatial variations of water temperature and net radiation were observed (Wang et al., 2014). Moreover, our issue with the 1-D lake models is their overestimation of the mixing, as discussed above. Adding unresolved horizontal mixing would not solve the issue. One common approach to account for the stratification effect in turbulence models is to include the stability function, which was deactivated in the control configuration for both UOM and SIMSTRAT. However, our sensitivity experiments showed that the incorporation of the stability function has nearly no effect on model performance (Figures S1–S4), which agrees with the conclusion from Goudsmit et al. (2002). Additional tests revealed that deactivating the bottom boundary effect on the turbulence scale also makes no difference in representing the thermal structure in Lake Taihu (Figures S1 and S3).

Alternatively, another effective method to account for the stratification effect is to directly tune Pr_t (Dunckley et al., 2012; Noh et al., 2005; Ye et al., 2019). Actually, Pr_t is commonly regarded as a tunable parameter both in 1-D lake models like SIMSTRAT and 3-D hydrodynamic models like FVCOM. In the neutral condition, Pr_t is typically set to around 1. However, Pr_t varies to a great extent in aquatic systems (Goodman & Levine, 2003; Muench et al., 2009), and generally increases as the stable stratification intensifies. Elliott

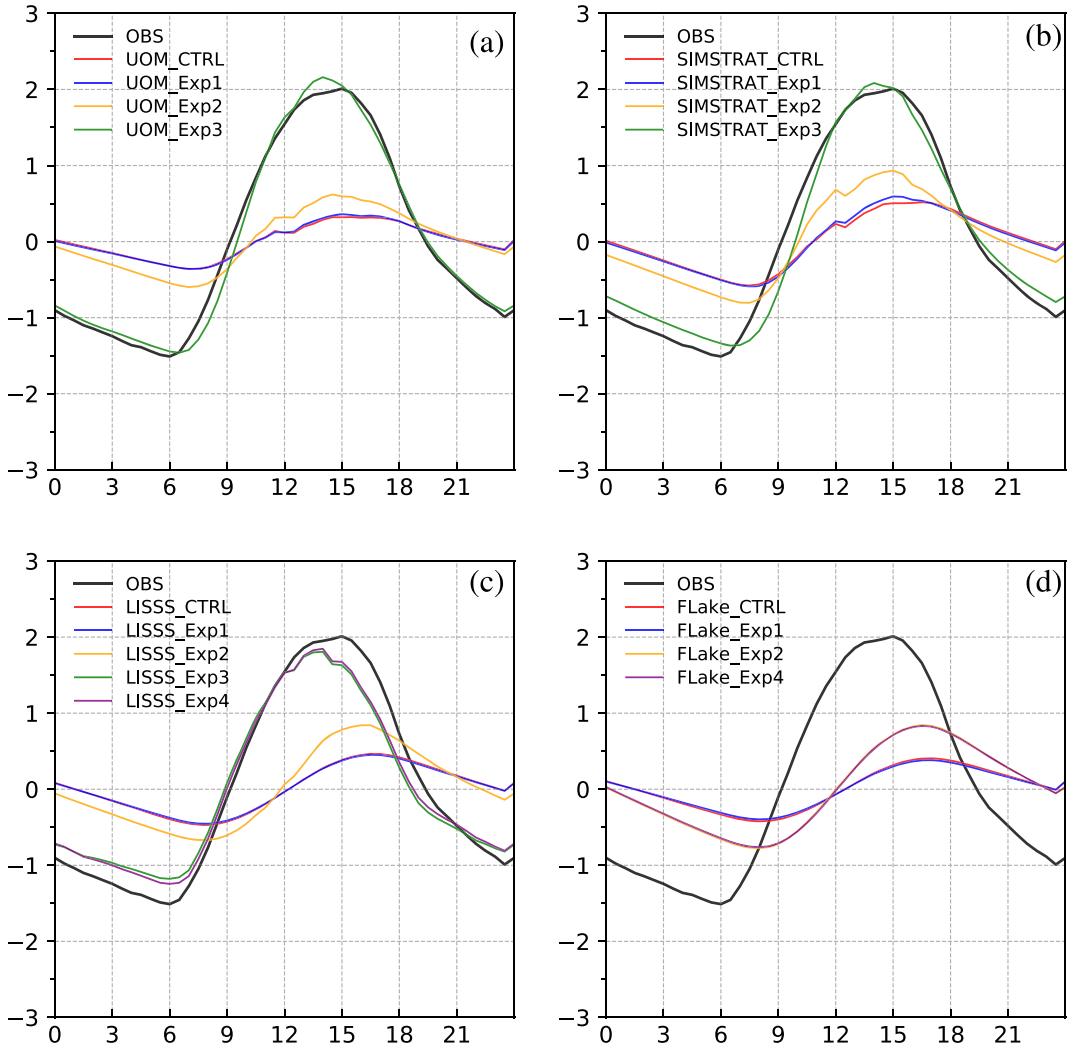

Figure 8. Averaged diurnal cycle of LST observed (black) and simulated from control and sensitivity experiments for (a) UOM, (b) SIMSTRAT, (c) LISSS, and (d) FLake.

and Venayagamoorthy (2011) evaluated four Pr_t parameterizations for stably stratified flows. Their Pr_t values vary between 0.8 and 3.0 (4.6–18.7) when the gradient Richardson number (R_i) equals to 0.25 (3.0). Lake Taihu commonly experiences extreme daytime stratification especially in summer season due to its great shallowness. However, the default neutral value of Pr_t is obviously too small and not appropriate for the application in Lake Taihu. As a result, increasing Pr_t is a reasonable approach to account for the restriction of strong stratification on the vertical mixing.

In Exp3, which included both the Exp1 and Exp2 changes, Pr_t was increased from 1 to 20 to reduce the vertical turbulent mixing. The diffusivity ν_h now fell on the order of 2.5×10^{-5} m^2 s^{-1}, which was similar to the finding by Xu et al. (2016) for Lake Erhai. Consequently, UOM was able to produce a much more realistic time evolution of LST as well as water temperature at the 20 cm depth. The LST rmse was reduced from 1.45°C to 0.82°C and temporal correlation with observations increased from 0.93 to 0.98. Thus, with this restricted mixing, UOM successfully reproduced the observed LST diurnal range, with accurate timing of both the peak and valley (Figure 8a). Note that the two abnormal LST peaks on 13 and 25 August 2012 stemmed from likely spurious low wind speeds, which were constant 0.2 m s^{-1} during most of the day and obviously disagreed with the diurnal distribution typically observed (Figure 2a) as well as obviously contradicted to other observation sites (not shown). Moreover, the differences in the simulated lake current

profile among the experiments are not obvious (not shown). The model responds very quickly to the change of surface wind forcing due to the shallowness of Lake Taihu.

In accordance with UOM, the k-ε turbulence model SIMSTRAT showed a similar sensitivity to the increases of Pr_t (Figure 4), except for frequent LST overestimations (Figure 4a) in sunny and calm days (disregarding the likely spurious observations). The exception occurred because of extremely low thermal diffusivities (as compared to UOM) in such weather conditions, which caused solar heat to build up in the surface layer. Additional tests, decreasing solar absorption coefficient β to lower values such as 0.5, could alleviate the heat built-up but deteriorate the performance in representing the LST diurnal cycle. Moreover, SIMSTRAT has three empirical constants: shear production ($\varepsilon_1 = 1.44$), dissipation ($\varepsilon_2 = 1.92$), and buoyancy ($\varepsilon_3 = -0.4$ in case of stratification) in the ε equation. As expected, its model performance is sensitive only to ε_3 as related to stratification. To clarify its effect, we conducted three experiments SIMSTRAT_Exp2-c3-0.1, SIMSTRAT_Exp2-c3-10, and SIMSTRAT_Exp2-c3-100 similar to SIMSTRAT_Exp2 except for multiplying ε_3 by 0.1, 10, and 100, respectively. Figure S5 shows that the diurnal amplitude increases as a larger ε_3 is used. By an increase of 100 times, SIMSTRAT_Exp2-c3-100 can produce a reasonable LST diurnal cycle, but its performance is still worse than SIMSTRAT_Exp3. Figure S6 compares the overall performance between SIMSTRAT_Exp3 and SIMSTRAT_Exp2-c3-100 using the Taylor diagram. It shows that SIMSTRAT_Exp3 outperforms SIMSTRAT_Exp2-c3-100 in simulating the LST and water temperatures at each probing depth. Therefore, the restriction of heat transfer from stable stratification may be realized by tuning Pr_t or empirical constant ε_3. Note that for different applications of the standard k-ε model in oceans and lakes, such empirical parameters are generally fixed except for $c_\mu^{'}$, which is set as c_μ divided by Pr_t to parameterize the dependence on Pr_t (Burchard, 2002). This is the same for UOM application (Ling et al., 2015; Noh et al., 2005). Accordingly, we only tune Pr_t while keeping other empirical parameters unchanged in both SIMSTRAT and UOM.

To test the effectiveness of the Pr_t parameterizations noted in Elliott and Venayagamoorthy (2011), for both UOM and SIMSTRAT we conducted four experiments similar to Exp2 except using different schemes: Exp2_KM (Kim & Mahrt, 1992), Exp2_PGT (Peters et al., 1988), Exp2_VS (Venayagamoorthy & Stretch, 2010), and Exp2_MA (Munk & Anderson, 1948). Among these four schemes, KM yielded the best skill (Figure S7), and improved over Exp2 to increase the LST diurnal amplitude by 1.17°C and 0.86°C in UOM and SIMSTRAT respectively. However, its skill was still worse than Exp3 and significantly underestimated the diurnal cycle. Therefore, a physical parameterization may be more desirable to account for the stratification effect than the stability function, and setting Pr_t to a constant 20 is adequate for shallow lakes.

For LISSS, previous studies (Deng et al., 2013; Subin et al., 2012; Xu et al., 2016) showed that the default wind-driven eddy diffusion parameterization of Hostetler and Bartlein (1990) often overpredicts the mixing process in shallow lakes, leading to a suppressed LST diurnal range. As a common practice for recent lake modeling using LISSS, the parametrized eddy diffusivity coefficient was subjectively enhanced (reduced) by a factor in the order of 10–100 to account for the strong (weak) vertical mixing process in the deep (shallow) lakes (Deng et al., 2013; Gu et al., 2015; Huang et al., 2019; Xu et al., 2016). Following Deng et al. (2013), we reduced the eddy diffusivity by a factor of 0.01 to restrict the mixing. This enabled LISSS to realistically capture the LST diurnal cycle, having a correlation with observations of 0.97 and rmse of 0.67°C. However, LISSS produced unexpected large warm biases (1.6–1.7°C) at the depth of 20 and 50 cm (Figures 5b and 5c) when reducing the mixing factor. The result, in agreement with Deng et al. (2013), indicated that too much heat was built up near the surface and not efficiently transported to deeper layers. Compared to the turbulence models, LISSS needs a greater reduction in eddy diffusivity values to capture the LST diurnal cycle. This is mainly due to the inherent limitation of the wind-driven eddy diffusion parameterization, which makes LISSS unable to achieve a balance between a realistic LST diurnal range and reasonable upper-layer water temperatures in Lake Taihu for summer. When increasing Pr_t in the turbulence models, UOM and SIMSTRAT, the performance at each probing depth was either improved or unchanged (Figure 7).

No modification on the vertical mixing was tested in FLake since the model was designed as calibration-free using the self-similarity theory and adjustable only for external parameters including lake depth, fetch, and light extinction coefficient.

4.2.4. Bottom Sediment

For shallow lakes, the heat transfer has been identified to occur between the water body and underlying sediments (Fang & Stefan, 1996, 1998). FLake and LISSS both include a sediment thermal scheme to explicitly resolve this heat transfer. In Exp4, the underlying thermal submodel in both FLake and LISSS was deactivated (i.e., using no-flux condition) to identify the effect of the sediments on the lake thermal structure. The removal of sediments in FLake had little impact either on the water layers immediately adjacent to the lake bottom and nor to the LST performance (Figure 6). In LISSS, the effect was also very minor in summer because the water is highly stratified through strong solar heating. In cold days during autumn, the heat transfer from the sediments could warm adjacent bottom layers by 0.5°C (increasing the bias) but still had minor effects on LST (Figure 5). This result, in agreement with Stepanenko et al. (2013), suggests that the sediment effect is minor to LST and the upper layer thermal structure.

4.2.5. Independent Evaluation

To test the applicability of the modified UOM, sensitivity experiments by gradually using the proposed tuning approaches (in terms of roughness, extinction, and mixing) were also conducted at three other measurement sites (i.e., BFG, PTS, and XLS). Figures S8–S10 present the simulated half-hourly series of LST and water temperatures at each probing depth from 1 August to 30 September 2013, while Figure S11 compares their overall performance using the Taylor diagram. The UOM with its control configuration presents substantial cold biases in the whole water column at all these three sites, similar to the focus site. The inclusion of parameterized roughness lengths and enhanced radiation absorption improved the model performance by reducing cold biases, but still considerably underestimated the LST diurnal range (Figure S12). When increasing Pr_t to 20, Exp3 could reproduce the realistic LST diurnal cycle for all measurement sites, leading to improved skill in simulating LST and water temperatures at each depth. These results indicate that our proposed UOM refinements are generally applicable for shallow lakes.

5. Model Intercomparison

Given the localization through the sensitivity analysis presented above, each model has substantially improved its performance in simulating the thermal structure of Lake Taihu, especially for the LST diurnal cycle and seasonal variation. The recommended configuration for the best performance is respectively UOM-Exp3, SIMSTRAT-Exp3, LISSS-Exp3, and FLake-Exp2. These configurations were all integrated throughout year 2013, providing a validation period independent of year 2012 in which the models were tuned. The results were intercompared below, focusing on the summer (from 1 June to 31 August) and autumn (from 1 September to 30 November) in which two distinct thermal regimes prevailed due to strong and weak stratifications, respectively.

5.1. Summer Regime

Figure 9a compares the summer daily mean LST time series observed and simulated by the four tuned lake model configurations, while Figure 10 depicts their overall performances using the Taylor diagram. All four models realistically represented the LST temporal variations. For instance, the warming trend of LST during early summer were well captured. As compared with observations, UOM, SIMSTRAT, LISSS, and FLake produced a correlation coefficient of respectively 0.99, 0.98, 0.99, and 0.96, and rmse of 0.76°C, 0.81°C, 0.92°C, and 1.11°C. Overall, UOM performed the best.

However, systematic model peculiarities were evident. Figure 11 illustrates these using boxplots of the simulated LST biases, including the median, the 25th and 75th percentiles, and their extremes. UOM produced a relatively narrow middle range of biases with the median located near 0, indicating its good skill in simulating LST variations. LISSS produced an even narrower middle range of biases, but that range was entirely located under zero, indicating systematic cold biases. SIMSTRAT had not only the middle range larger than both UOM and LISSS (although its median located near zero) but also higher extreme values as discussed earlier. FLake was the worst performer, simulated a much wider middle range and greater extremes than other models.

The seasonal average LST diurnal cycle also revealed significant intermodel variations (Figure 12a). The observed diurnal range was approximately 3.7°C, with the peak and valley occurred at 1500 and 0530 local time. UOM most realistically reproduced the diurnal cycle in both phase and magnitude. While SIMSTRAT produced a similarly good diurnal cycle on average, its result was less realistic (than UOM) due to the

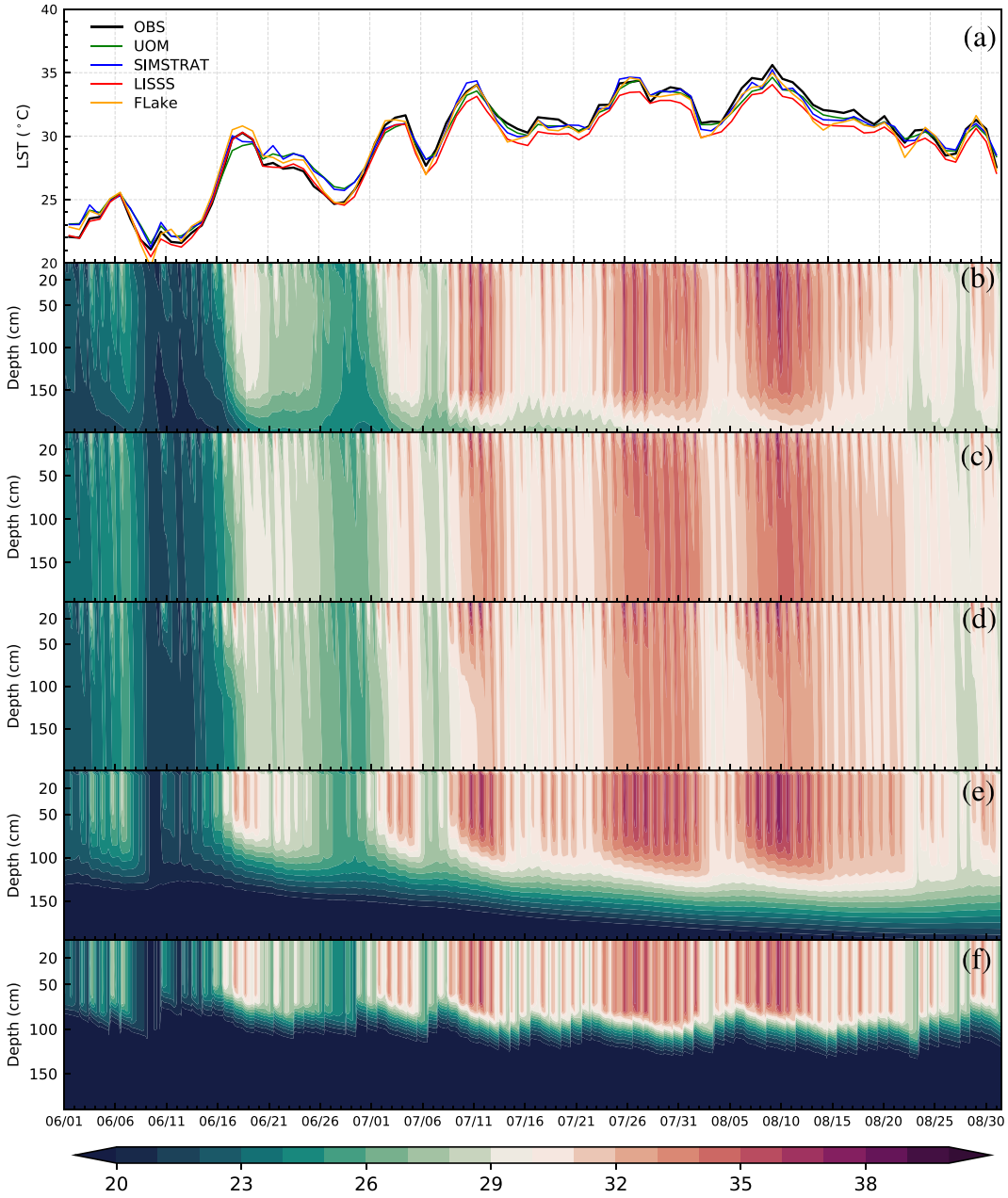

Figure 9. Comparison of daily mean LST time series (a) and time-depth distributions of water temperatures from (b) observations, (c) UOM, (d) SIMSTRAT, (e) LISSS, and (f) FLake during summer 2013.

compensation from the frequent strikes (i.e., high extreme warm biases) identified earlier. On the other hand, LISSS underestimated the diurnal range by 0.3°C (mainly due to a lower peak) along with a systematic phase shift by 1 hr earlier between 0800–2000. FLake was the worst, underestimating the diurnal range by 0.7°C (due to a lower peak) along with a systematic phase delay by 2 hr.

Figures 9b–9f compares water temperature profiles among observations and simulations by the four tuned lake models. The evolution of the observed vertical thermal structure (Figure 9b) was highly related to the meteorological forcing variation. Starting from early July, the lake water stratification was enhanced as solar radiation and air temperature increased. Intermittent occurrences of increased wind speed or decreased solar radiation in cloudy days destabilized the water column. UOM (Figure 9c) well represented these lake thermal structure responses to changing weather conditions. Its good performance was also reflected as

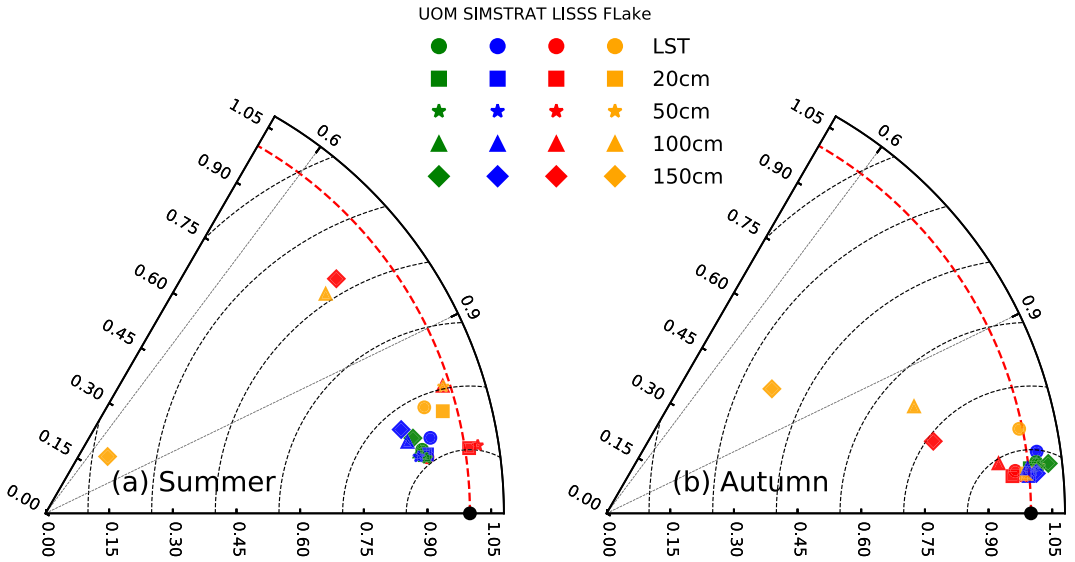

Figure 10. Taylor diagram of pattern statistics comparing overall performances of 1-D lake models in simulating the LST and water temperatures (20, 50, 100, and 150 cm) during (a) summer and (b) autumn 2013.

higher skill scores in the Taylor diagram (Figure 10). The model somewhat overestimated the extent of stratification and misrepresented the thermal structure near the lake bottom. This resulted from the absence of the bottom sediment effect. SIMSTRAT (Figure 9d), the other turbulence closure model, performed a little worse, slightly overestimating the stratification in the upper layers and reversely below in warm days. This caused its warm biases in LST and near-surface layers and cold biases below.

LISSS (Figure 9e) exaggerated even more (than SIMSTRAT) the daytime stratification in the upper water column as noted previously. It also overestimated the duration of the daytime stratification. This led to stronger (than observed) temperature gradients in the mixed layer, accompanied with large cold biases in the lower layers. These biases resulted from the compensation of reducing the diffusivity (for vertical mixing) in order to better represent the LST diurnal range. FLake (Figure 9f) performed the worst and its skill score got lower as the lake depth increases, producing substantial cold biases below 50 cm (Figure 10a). Stepanenko et al. (2013) reported that FLake produced severe cold biases in the midlatitude, shallow Lake Kossenblatter See, as a result of the intensive stratification typical in summer. FLake applications are known to be sensitive to the lake depth and not suitable for deep lakes (>50 m) unless using a "virtual bottom" (Huang et al., 2019; Martynov et al., 2010). Our study further discourages FLake application for very shallow lakes (<5 m) in warm seasons.

5.2. Autumn Regime

From summer to autumn, the sign of the water surface to air temperature difference is usually reversed (from negative to positive) over large dimictic lakes, such as the Great Lakes (Blanken et al., 2011; Lofgren & Zhu, 2000), which increases the instability of the atmospheric boundary layer and thus enlarges the turbulent fluxes into the atmosphere. In Lake Taihu, surface temperature is warmer than the overlying air temperature in most times of the year and the upward heat fluxes in general decrease as air temperature declines (Wang et al., 2014). As such, the cooling of Lake Taihu in autumn is mainly driven by the reduction of the surface net radiation, more so than in summer.

Figure 13a compares the autumn daily mean LST time series observed and simulated by the four tuned lake model configurations. All models well captured the declining LST trend since 25 September. On average, the observed diurnal range was approximately 3.0°C, with the peak and valley occurred at 1430 and 0630 local time (Figure 12b). Overall, UOM best captured the observed diurnal cycle in both phase and magnitude. SIMSTRAT underestimated the diurnal range by 0.35°C, with systematically warmer nighttime and cooler daytime biases, while delayed the morning warming phase by 1 hr. On the other hand, LISSS shifted the

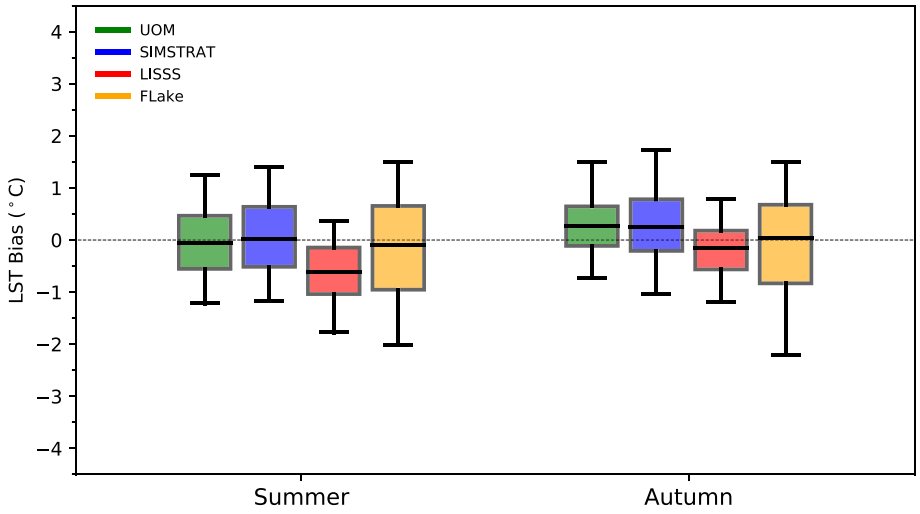

Figure 11. The boxplot of the simulated LST biases (MODEL-OBS) for summer and autumn 2013.

peak and the whole warm phase between 0900–2000 by 1 hr earlier than observations. FLake performed the worst, not only substantially underestimated the diurnal range (by 1.5°C) but also delayed the cycle systematically by 1.5 hr.

As compared to the summer, diurnal overturn was observed to still occur while the daytime stratification gradually weakened in the autumn (Figure 13b). Both UOM and SIMSTRAT well captured the evolution of the thermal structure above 150 cm (Figures 13c and 13d), with high skill scores at each depth (Figure 10b). An inverse temperature layer emerged in late October below 150 cm as the direction of heat flux between the water and underlying sediment reversed in cold seasons. No model, even LISSS and FLake with explicit sediment treatments, could simulate this inversion. LISSS improved over summer in simulating the vertical thermal structure in autumn characterized by weaker stratification, but still overestimated the thermal gradients near 150 cm. FLake was still inferior to other models in modeling the vertical structure.

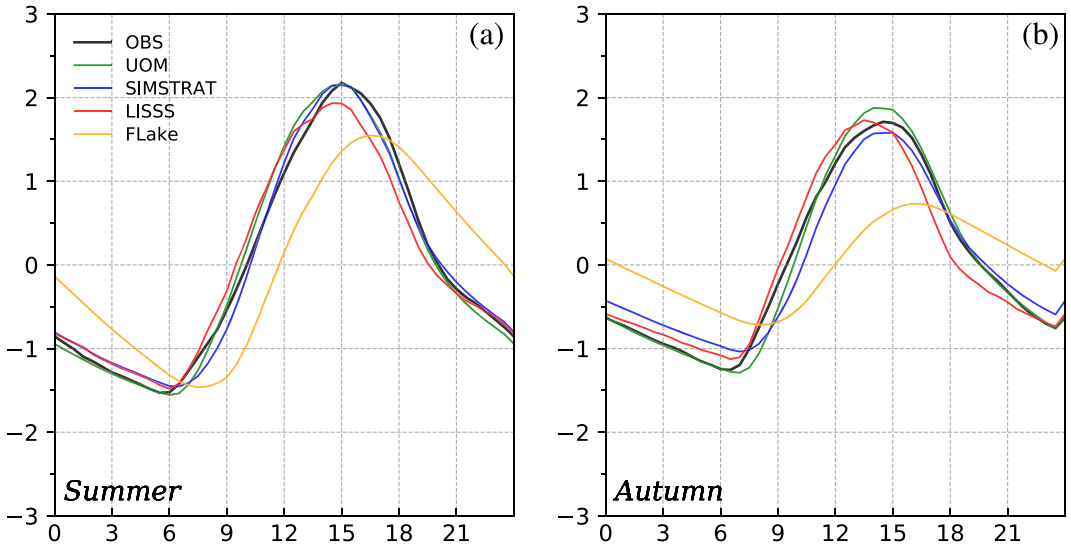

Figure 12. Averaged diurnal cycle of LST observed (black) and simulated by 1-D lake models during (a) summer and (b) autumn 2013.

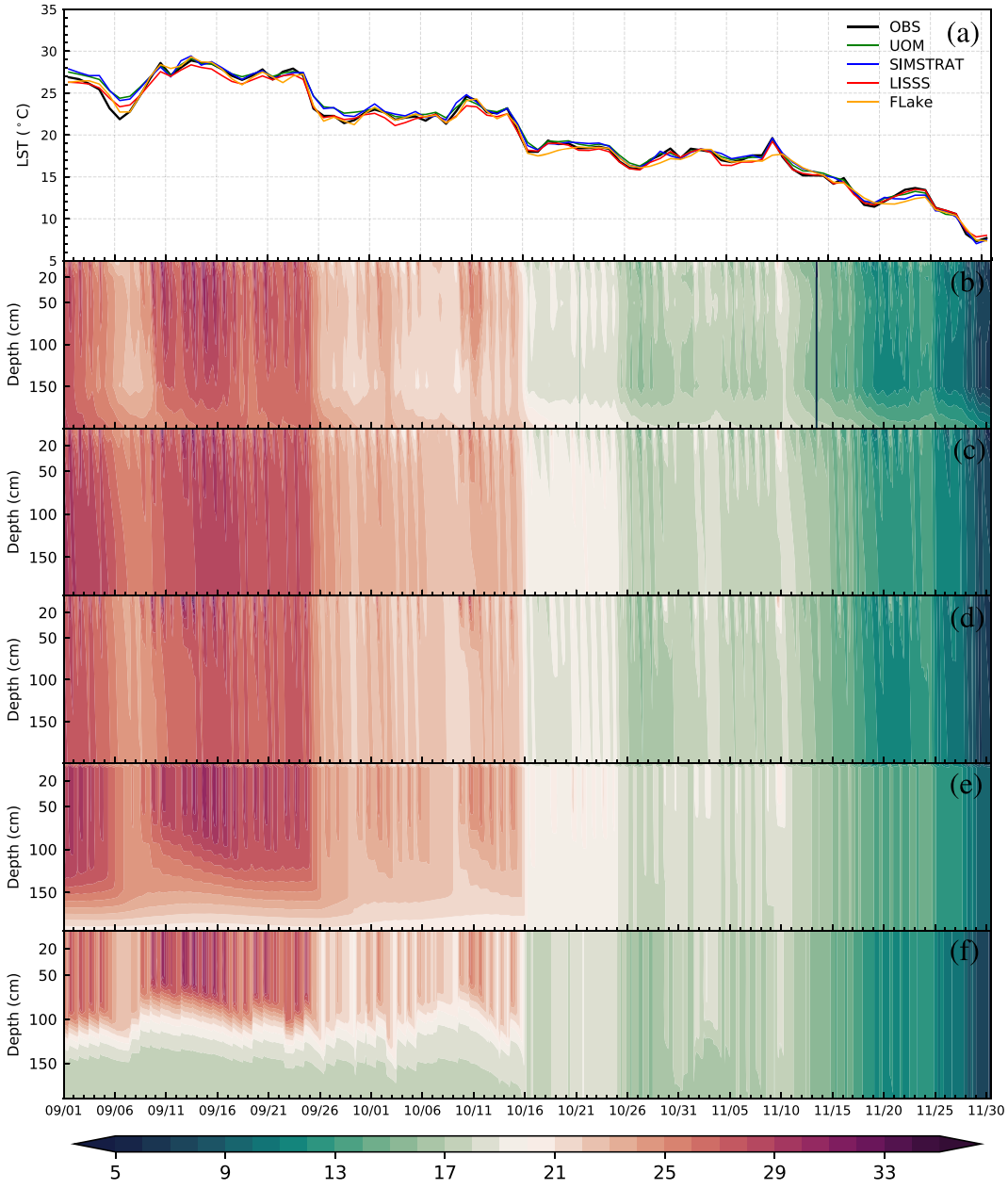

Figure 13. Same as Figure 9 except for autumn.

6. Summary and Conclusions

In this study, a multilevel UOM developed by Ling et al. (2015) on the basis the simple one-equation TKE closure scheme (Noh, 1996; Noh & Jin Kim, 1999; Noh et al., 2011) was customized for application to shallow lakes. This modified UOM together with three other popular 1-D lake models, SIMSTRAT, LISSS, and FLake, was first systematically tested against comprehensive eddy covariance measurements in the large, shallow Lake Taihu. The surface flux scheme (Oleson et al., 2013; Zeng et al., 1998) was incorporated into all the models to eliminate their discrepancies in representing atmosphere-lake exchanges.

All models in their default configurations produced substantial cold biases in lake water temperatures and significantly underestimated LST diurnal range. Implementing a new parametrization of surface roughness lengths (Subin et al., 2012; Zilitinkevich et al., 2001) considerably diminished the excessive turbulence heat fluxes and thus significantly reduced the cold biases. Employing a simple solar penetration formula with

increased light extinction coefficient and surface absorption fraction further reduced the cold biases in LST and the water column. Reducing the turbulent mixing strength by increasing Pr_t to 20 in UOM and SIMSTRAT and decreasing the mixing factor to 0.01 in LISSS enabled these models to capture the observed LST diurnal range with realistic stratification and turnover. Removing sediments showed a minor effect on the thermal structure near the lake bottom in LISSS but less effect in FLake, and both of these had little impact on the LST simulation. Additional tests at other three measurement sites further demonstrate the effectiveness of these modifications and the general applicability of the improved UOM for shallow lakes.

After adopting the three new treatments, that is, surface roughness, solar penetration, and turbulent mixing, these tuned models were intercompared against in situ measurements in the same Lake Taihu but in the year 2013, independent of the year 2012 used in modeling tuning. Among all models, UOM most realistically captured the LST diurnal cycle and the evolution of the lake thermal structure under both strong and weak stratifications in summer and autumn, respectively. SIMSTRAT performed less accurately, with frequent LST spikes (i.e., large warm biases) as a result of the extremely low thermal diffusivities in sunny and calm days. LISSS shifted the LST diurnal cycle by about 1 hr in both seasons, and could not achieve a balance between a realistic LST diurnal range and reasonable upper-layer water temperatures in summer. FLake performed the worst, not only substantially underestimated the LST diurnal range and delayed phase by 1.5–2 hr but also poorly simulated the lake thermal structure.

In conclusion, the UOM customized in this study is well suited for application to shallow lakes. Further research is needed to evaluate its performance and additional improvements required for application to deep lakes. In particular, the snow and ice processes, which were not presently accounted, must be incorporated to facilitate its utility for high-latitude lakes.

Data Availability Statement

Observational data and model simulations used in this study is accessible online (ftp://earthserver.umd.edu/publish).

Acknowledgments

We acknowledge two anonymous reviewers for their constructive comments and suggestions for improving the manuscript. The research was supported by the National Key Research and Development Program of China grant to Ling (2016YFC1401400), the Jiangsu Institute of Meteorological Sciences subcontract (NJCAR2016ZD03), and the China Meteorological Administration/National Climate Center research subcontract (2211011816501) both to Nanjing University of Information Science and Technology, and the China Scholar Council fellowship to Sun for his visit at the University of Maryland. Liang was partially supported by U.S. National Science Foundation Innovations at the Nexus of Food, Energy and Water Systems under Grant EAR1903249. The simulations and analyses were conducted on supercomputers, including the Maryland Advanced Research Computing Center's Bluecrab and the Computational and Information Systems Lab of the National Center for Atmospheric Research.

References

Axell, L. B., & Liungman, O. (2001). A one-equation turbulence model for geophysical applications: Comparison with data and the *k-ε* model. *Environmental Fluid Mechanics*, *1*(1), 71–106. https://doi.org/10.1023/A:1011560202388

Bai, X., Wang, J., Schwab, D. J., Yang, Y., Luo, L., Leshkevich, G. A., & Liu, S. (2013). Modeling 1993–2008 climatology of seasonal general circulation and thermal structure in the Great Lakes using FVCOM. *Ocean Modelling*, *65*, 40–63. https://doi.org/10.1016/j.ocemod.2013.02.003

Bennington, V., Notaro, M., & Holman, K. D. (2014). Improving climate sensitivity of deep lakes within a regional climate model and its impact on simulated climate. *Journal of Climate*, *27*(8), 2886–2911. https://doi.org/10.1175/JCLI-D-13-00110.1

Blanken, P. D., Spence, C., Hedstrom, N., & Lenters, J. D. (2011). Evaporation from Lake Superior: 1. Physical controls and processes. *Journal of Great Lakes Research*, *37*(4), 707–716. https://doi.org/10.1016/j.jglr.2011.08.009

Bonan, G. B. (1995). Sensitivity of a GCM simulation to inclusion of inland water surfaces. *Journal of Climate*, *8*(11), 2691–2704. https://doi.org/10.1175/1520-0442(1995)008<2691:SOAGST>2.0.CO;2

Burchard, H. (2002). *Applied turbulence modelling in marine waters* (Vol. 100). New York: Springer.

Burchard, H., Petersen, O., & Rippeth, T. P. (1998). Comparing the performance of the Mellor-Yamada and the *k-ε* two-equation turbulence models. *Journal of Geophysical Research*, *103*(C5), 10,543–10,554. https://doi.org/10.1029/98JC00261

Charusombat, U., Fujisaki-Manome, A., Gronewold, A. D., Lofgren, B. M., Anderson, E. J., Blanken, P. D., et al. (2018). Evaluating and improving modeled turbulent heat fluxes across the North American Great Lakes. *Hydrology and Earth System Sciences*, *22*(10), 5559–5578. https://doi.org/10.5194/hess-22-5559-2018

Chen, C., Liu, H., & Beardsley, R. C. (2003). An unstructured grid, finite-volume, three-dimensional, primitive equations ocean model: Application to coastal ocean and estuaries. *Journal of Atmospheric and Oceanic Technology*, *20*(1), 159–186. https://doi.org/10.1175/1520-0426(2003)020<0159:AUGFVT>2.0.CO;2

Deng, B., Liu, S., Xiao, W., Wang, W., Jin, J., & Lee, X. (2013). Evaluation of the CLM4 lake model at a large and shallow freshwater lake. *Journal of Hydrometeorology*, *14*(2), 636–649. https://doi.org/10.1175/JHM-D-12-067.1

Diallo, I., Giorgi, F., & Stordal, F. (2018). Influence of Lake Malawi on regional climate from a double-nested regional climate model experiment. *Climate Dynamics*, *50*(9–10), 3397–3411. https://doi.org/10.1007/s00382-017-3811-x

Donner, L. J., Wyman, B. L., Hemler, R. S., Horowitz, L. W., Ming, Y., Zhao, M., et al. (2011). The dynamical core, physical parameterizations, and basic simulation characteristics of the atmospheric component AM3 of the GFDL global coupled model CM3. *Journal of Climate*, *24*(13), 3484–3519. https://doi.org/10.1175/2011JCLI3955.1

Dunckley, J. F., Koseff, J. R., Steinbuck, J. V., Monismith, S. G., & Genin, A. (2012). Comparison of mixing efficiency and vertical diffusivity models from temperature microstructure. *Journal of Geophysical Research*, *117*, C10008. https://doi.org/10.1029/2012JC007967

Dupont, F., Chittibabu, P., Fortin, V., Rao, Y. R., & Lu, Y. (2012). Assessment of a NEMO-based hydrodynamic modelling system for the Great Lakes. *Water Quality Research Journal*, *47*(3–4), 198–214. https://doi.org/10.2166/wqrjc.2012.014

Dutra, E., Stepanenko, V. M., Balsamo, G., Viterbo, P., Miranda, P., Mironov, D., & Schär, C. (2010). An offline study of the impact of lakes on the performance of the ECMWF surface scheme. *Boreal Environment Research*, *15*, 100–112.

Elliott, Z. A., & Venayagamoorthy, S. K. (2011). Evaluation of turbulent Prandtl (Schmidt) number parameterizations for stably stratified environmental flows. *Dynamics of Atmospheres and Oceans*, *51*(3), 137–150. https://doi.org/10.1016/j.dynatmoce.2011.02.003

Fang, X., & Stefan, H. G. (1996). Dynamics of heat exchange between sediment and water in a lake. *Water Resources Research*, *32*(6), 1719–1727. https://doi.org/10.1029/96WR00274

Fang, X., & Stefan, H. G. (1998). Temperature variability in lake sediments. *Water Resources Research*, *34*(4), 717–729. https://doi.org/10.1029/97WR03517

Galperin, B., Kantha, L. H., Hassid, S., & Rosati, A. (1988). A quasi-equilibrium turbulent energy model for geophysical flows. *Journal of the Atmospheric Sciences*, *45*(1), 55–62. https://doi.org/10.1175/1520-0469(1988)045<0055:AQETEM>2.0.CO;2

Gaudard, A., Schwefel, R., Vinnå, L. R., Schmid, M., Wüest, A., & Bouffard, D. (2017). Optimizing the parameterization of deep mixing and internal seiches in one-dimensional hydrodynamic models: A case study with Simstrat v1. 3. *Geoscientific Model Development*, *10*(9), 3411–3423. https://doi.org/10.5194/gmd-10-3411-2017

Goodman, L., & Levine, E. R. (2003). Use of turbulent kinetic energy and scalar variance budgets to obtain directly eddy viscosity and diffusivity from AUV turbulence measurements. https://www.semanticscholar.org/paper/Use-of-Turbulent-Kinetic-Energy-and-Scalar-Variance-Goodman-Levine/3aaa3e6a586d661a4a6d0550d116c59de3d1841d

Goudsmit, G.-H., Burchard, H., Peeters, F., & Wüest, A. (2002). Application of k-ε turbulence models to enclosed basins: The role of internal seiches. *Journal of Geophysical Research*, *107*(C12), 3230. https://doi.org/10.1029/2001JC000954

Goyette, S., McFarlane, N. A., & Flato, G. M. (2000). Application of the Canadian Regional Climate Model to the Laurentian Great Lakes region: Implementation of a lake model. *Atmosphere-Ocean*, *38*(3), 481–503. https://doi.org/10.1080/07055900.2000.9649657

Gu, H., Jin, J., Wu, Y., Ek, M. B., & Subin, Z. M. (2015). Calibration and validation of lake surface temperature simulations with the coupled WRF-lake model. *Climatic Change*, *129*(3–4), 471–483. https://doi.org/10.1007/s10584-013-0978-y

Gu, H., Shen, X., Jin, J., Xiao, W., & Wang, Y. W. (2013). An application of a 1-D thermal diffusion lake model to Lake Taihu. *Acta Meteorologica Sinica*, *71*, 719–730.

Haddout, S., Priya, K. L., Boko, M., & Azidane, H. (2018). Comparison of one-dimensional (1-D) column lake models prediction for surface water temperature in eight selected Moroccan lakes. *ISH Journal of Hydraulic Engineering*, *24*(3), 317–329. https://doi.org/10.1080/09715010.2017.1376294

Hakanson, L. (1995). Models to predict Secchi depth in small glacial lakes. *Aquatic Sciences*, *57*(1), 31–53. https://doi.org/10.1007/BF00878025

Henderson-Sellers, B. (1985). New formulation of eddy diffusion thermocline models. *Applied Mathematical Modelling*, *9*(6), 441–446. https://doi.org/10.1016/0307-904X(85)90110-6

Herb, W. R., & Stefan, H. G. (2005). Dynamics of vertical mixing in a shallow lake with submersed macrophytes. *Water Resources Research*, *41*, W02023. https://doi.org/10.1029/2003WR002613

Hostetler, S. W., & Bartlein, P. J. (1990). Simulation of lake evaporation with application to modeling lake level variations of Harney-Malheur Lake, Oregon. *Water Resources Research*, *26*(10), 2603–2612. https://doi.org/10.1029/WR026i010p02603

Hostetler, S. W., Bates, G. T., & Giorgi, F. (1993). Interactive coupling of a lake thermal model with a regional climate model. *Journal of Geophysical Research*, *98*(D3), 5045–5057. https://doi.org/10.1029/92JD02843

Huang, A., Lazhu, Wang, J., Dai, Y., Yang, K., Wei, N., et al. (2019). Evaluating and improving the performance of three 1-D Lake models in a large deep Lake of the Central Tibetan Plateau. *Journal of Geophysical Research: Atmospheres*, *124*, 3143–3167. https://doi.org/10.1029/2018JD029610

Huang, C. C., Li, Y. M., Le, C. F., Sun, D. Y., Wu, L., Wang, L. Z., & Wang, X. (2009). Seasonal characteristics of the diffuse attenuation coefficient of Meiliang Bay waters and its primary contributors. *Acta Ecologica Sinica*, *29*(6), 3295–3306.

Joehnk, K. D., & Umlauf, L. (2001). Modelling the metalimnetic oxygen minimum in a medium sized alpine lake. *Ecological Modelling*, *136*(1), 67–80. https://doi.org/10.1016/S0304-3800(00)00381-1

Kantha, L. H., & Clayson, C. A. (2000). *Small scale processes in geophysical fluid flows* (Vol. 67). London: Elsevier.

Kara, A. B., Wallcraft, A. J., & Hurlburt, H. E. (2005). A new solar radiation penetration scheme for use in ocean mixed layer studies: An application to the Black Sea using a fine-resolution Hybrid Coordinate Ocean Model (HYCOM). *Journal of Physical Oceanography*, *35*(1), 13–32. https://doi.org/10.1175/JPO2677.1

Kim, J., & Mahrt, L. (1992). Simple formulation of turbulent mixing in the stable free atmosphere and nocturnal boundary layer. *Tellus A*, *44*(5), 381–394. https://doi.org/10.1034/j.1600-0870.1992.t01-4-00003.x

Klein, P., & Coantic, M. (1981). A numerical study of turbulent processes in the marine upper layers. *Journal of Physical Oceanography*, *11*(6), 849–863. https://doi.org/10.1175/1520-0485(1981)011<0849:ANSOTP>2.0.CO;2

Lee, X., Liu, S., Xiao, W., Wang, W., Gao, Z., Cao, C., et al. (2014). The Taihu eddy flux network: An observational program on energy, water, and greenhouse gas fluxes of a large freshwater lake. *Bulletin of the American Meteorological Society*, *95*(10), 1583–1594. https://doi.org/10.1175/BAMS-D-13-00136.1

Liang, X.-Z., Sun, C., Zheng, X., Dai, Y., Xu, M., Choi, H. I., et al. (2018). CWRF performance at downscaling China climate characteristics. *Climate Dynamics*, *52*(3-4), 2159–2184. https://doi.org/10.1007/s00382-018-4257-5

Liang, X.-Z., Xu, M., Yuan, X., Ling, T., Choi, H. I., Zhang, F., et al. (2012). Regional climate–weather research and forecasting model. *Bulletin of the American Meteorological Society*, *93*(9), 1363–1387. https://doi.org/10.1175/BAMS-D-11-00180.1

Ling, T., Xu, M., Liang, X.-Z., Wang, J. X. L., & Noh, Y. (2015). A multilevel ocean mixed layer model resolving the diurnal cycle: Development and validation. *Journal of Advances in Modeling Earth Systems*, *7*, 1680–1692. https://doi.org/10.1002/2015MS000476

Lofgren, B. M., & Zhu, Y. (2000). Surface energy fluxes on the Great Lakes based on satellite-observed surface temperatures 1992 to 1995. *Journal of Great Lakes Research*, *26*(3), 305–314. https://doi.org/10.1016/S0380-1330(00)70694-0

Long, Z., Perrie, W., Gyakum, J., Caya, D., & Laprise, R. (2007). Northern lake impacts on local seasonal climate. *Journal of Hydrometeorology*, *8*(4), 881–896. https://doi.org/10.1175/JHM591.1

MacKay, M. D. (2012). A process-oriented small lake scheme for coupled climate modeling applications. *Journal of Hydrometeorology*, *13*(6), 1911–1924. https://doi.org/10.1175/JHM-D-11-0116.1

Martynov, A., Sushama, L., & Laprise, R. (2010). Simulation of temperate freezing lakes by one-dimensional lake models: Performance assessment for interactive coupling with regional climate models. *Boreal Environment Research*, *15*, 143–164.

Mcwilliams, J. C., Norton, N. J., Gent, P. R., & Haidvogel, D. B. (1990). A linear balance model of wind-driven, midlatitude ocean circulation. *Journal of Physical Oceanography*, *20*(9), 1349–1378. https://doi.org/10.1175/1520-0485(1990)020<1349:ALBMOW>2.0.CO;2

Mellor, G. L., & Yamada, T. (1982). Development of a turbulence closure model for geophysical fluid problems. *Reviews of Geophysics*, *20*(4), 851–875. https://doi.org/10.1029/RG020i004p00851

Mironov, D., Heise, E., Kourzeneva, E., Ritter, B., Schneider, N., & Terzhevik, A. (2010). Implementation of the lake parameterisation scheme FLake into the numerical weather prediction model COSMO. *Boreal Environment Research*, *15*, 218–230.
Muench, R., Padman, L., Gordon, A., & Orsi, A. (2009). A dense water outflow from the Ross Sea, Antarctica: Mixing and the contribution of tides. *Journal of Marine Systems*, *77*(4), 369–387. https://doi.org/10.1016/j.jmarsys.2008.11.003
Munk, W. H., & Anderson, E. R. (1948). Notes on a theory of the thermocline. *Journal of Marine Research*, *7*(3), 276–295.
Noh, Y. (1996). Dynamics of diurnal thermocline formation in the oceanic mixed layer. *Journal of Physical Oceanography*, *26*(10), 2183–2195. https://doi.org/10.1175/1520-0485(1996)026<2183:dodtfi>2.0.co;2
Noh, Y., & Fernando, H. J. S. (1991). A numerical study on the formation of a thermocline in shear-free turbulence. *Physics of Fluids A: Fluid Dynamics*, *3*(3), 422–426. https://doi.org/10.1063/1.858098
Noh, Y., & Jin Kim, H. (1999). Simulations of temperature and turbulence structure of the oceanic boundary layer with the improved near-surface process. *Journal of Geophysical Research*, *104*(C7), 15,621–15,634. https://doi.org/10.1029/1999JC900068
Noh, Y., Kang, Y. J., Matsuura, T., & Iizuka, S. (2005). Effect of the Prandtl number in the parameterization of vertical mixing in an OGCM of the tropical Pacific. *Geophysical Research Letters*, *32*, L23609. https://doi.org/10.1029/2005GL024540
Noh, Y., Lee, E., Kim, D.-H., Hong, S.-Y., Kim, M.-J., & Ou, M.-L. (2011). Prediction of the diurnal warming of sea surface temperature using an atmosphere-ocean mixed layer coupled model. *Journal of Geophysical Research*, *116*, C11023. https://doi.org/10.1029/2011JC006970
Notaro, M., Holman, K., Zarrin, A., Fluck, E., Vavrus, S., & Bennington, V. (2013). Influence of the Laurentian Great Lakes on regional climate. *Journal of Climate*, *26*(3), 789–804. https://doi.org/10.1175/JCLI-D-12-00140.1
Oleson, K. W., Lawrence, D. M., Bonan, G. B., Drewniack, B., Huang, M., Koven, C. D., et al. (2013). Technical description of version 4.5 of the Community Land Model (CLM) (Technical Note No. NCAR/TN-503+ STR). Boulder, CO: National Center for Atmospheric Research Earth System Laboratory. https://doi.org/10.5065/D6RR1W7M
Perroud, M., Goyette, S., Martynov, A., Beniston, M., & Annevillec, O. (2009). Simulation of multiannual thermal profiles in deep Lake Geneva: A comparison of one-dimensional lake models. *Limnology and Oceanography*, *54*(5), 1574–1594. https://doi.org/10.4319/lo.2009.54.5.1574
Persson, P.-E. (1983). Off-flavours in aquatic ecosystems—An introduction. *Water Science and Technology*, *15*(6–7), 1–11. https://doi.org/10.2166/wst.1983.0125
Peters, H., Gregg, M. C., & Toole, J. M. (1988). On the parameterization of equatorial turbulence. *Journal of Geophysical Research*, *93*(C2), 1199–1218. https://doi.org/10.1029/JC093iC02p01199
Samuelsson, P., Kourzeneva, E., & Mironov, D. (2010). The impact of lakes on the European climate as simulated by a regional climate model. *Boreal Environment Research*, *15*, 113–129.
Schmid, M., & Köster, O. (2016). Excess warming of a Central European lake driven by solar brightening. *Water Resources Research*, *52*, 8103–8116. https://doi.org/10.1002/2016WR018651
Sharma, A., Hamlet, A. F., Fernando, H. J. S., Catlett, C. E., Horton, D. E., Kotamarthi, V. R., et al. (2018). The need for an integrated land-lake-atmosphere modeling system, exemplified by North America's Great Lakes region. *Earth's Future*, *6*, 1366–1379. https://doi.org/10.1029/2018EF000870
Stepanenko, V., Goyette, S., Martynov, A., Perroud, M., Fang, X., & Mironov, D. (2010). First steps of a lake model intercomparison project: LakeMIP. *Boreal Environment Research*, *15*, 191–202.
Stepanenko, V., Jöhnk, K. D., Machulskaya, E., Perroud, M., Subin, Z., Nordbo, A., et al. (2014). Simulation of surface energy fluxes and stratification of a small boreal lake by a set of one-dimensional models. *Tellus A: Dynamic Meteorology and Oceanography*, *66*, 21389. https://doi.org/10.3402/tellusa.v66.21389
Stepanenko, V., Mammarella, I., Ojala, A., Miettinen, H., Lykosov, V., & Vesala, T. (2016). LAKE 2.0: A model for temperature, methane, carbon dioxide and oxygen dynamics in lakes. *Geoscientific Model Development*, *9*(5), 1977–2006. https://doi.org/10.5194/gmd-9-1977-2016
Stepanenko, V., Martynov, A., Jöhnk, K. D., Subin, Z. M., Perroud, M., Fang, X., et al. (2013). A one-dimensional model intercomparison study of thermal regime of a shallow, turbid midlatitude lake. *Geoscientific Model Development*, *6*(4), 1337–1352. https://doi.org/10.5194/gmd-6-1337-2013
Strong, C., Kochanski, A. K., & Crosman, E. T. (2014). A slab model of the Great Salt Lake for regional climate simulation. *Journal of Advances in Modeling Earth Systems*, *6*, 602–615. https://doi.org/10.1002/2014MS000305
Subin, Z. M., Riley, W. J., & Mironov, D. (2012). An improved lake model for climate simulations: Model structure, evaluation, and sensitivity analyses in CESM1. *Journal of Advances in Modeling Earth Systems*, *4*, M02001. https://doi.org/10.1029/2011MS000072
Taylor, K. E. (2001). Summarizing multiple aspects of model performance in a single diagram. *Journal of Geophysical Research*, *106*(D7), 7183–7192. https://doi.org/10.1029/2000JD900719
Thiery, W., Davin, E. L., Panitz, H.-J., Demuzere, M., Lhermitte, S., & Van Lipzig, N. (2015). The impact of the African Great Lakes on the regional climate. *Journal of Climate*, *28*(10), 4061–4085. https://doi.org/10.1175/JCLI-D-14-00565.1
Thiery, W., Stepanenko, V. M., Fang, X., Jöhnk, K. D., Li, Z., Martynov, A., et al. (2014). LakeMIP Kivu: Evaluating the representation of a large, deep tropical lake by a set of one-dimensional lake models. *Tellus A: Dynamic Meteorology and Oceanography*, *66*, 21390. https://doi.org/10.3402/tellusa.v66.21390
Venayagamoorthy, S. K., & Stretch, D. D. (2010). On the turbulent Prandtl number in homogeneous stably stratified turbulence. *Journal of Fluid Mechanics*, *644*, 359–369. https://doi.org/10.1017/S002211200999293X
Wang, W., Xiao, W., Cao, C., Gao, Z., Hu, Z., Liu, S., et al. (2014). Temporal and spatial variations in radiation and energy balance across a large freshwater lake in China. *Journal of Hydrology*, *511*, 811–824. https://doi.org/10.1016/j.jhydrol.2014.02.012
Xu, L., Liu, H., Du, Q., & Wang, L. (2016). Evaluation of the WRF-lake model over a highland freshwater lake in southwest China. *Journal of Geophysical Research: Atmospheres*, *121*, 13,989–14,005. https://doi.org/10.1002/2016JD025396
Xu, Q., Chen, W., & Gao, G. (2008). Seasonal variations in microcystin concentrations in Lake Taihu, China. *Environmental Monitoring and Assessment*, *145*(1–3), 75–79. https://doi.org/10.1007/s10661-007-0016-5
Xue, P., Pal, J. S., Ye, X., Lenters, J. D., Huang, C., & Chu, P. Y. (2017). Improving the simulation of large lakes in regional climate modeling: Two-way lake–atmosphere coupling with a 3D hydrodynamic model of the Great Lakes. *Journal of Climate*, *30*(5), 1605–1627. https://doi.org/10.1175/JCLI-D-16-0225.1
Yao, H., Samal, N. R., Joehnk, K. D., Fang, X., Bruce, L. C., Pierson, D. C., et al. (2014). Comparing ice and temperature simulations by four dynamic lake models in Harp Lake: Past performance and future predictions. *Hydrological Processes*, *28*(16), 4587–4601. https://doi.org/10.1002/hyp.10180
Ye, X., Anderson, E. J., Chu, P. Y., Huang, C., & Xue, P. (2019). Impact of water mixing and ice formation on the warming of Lake Superior: A model-guided mechanism study. *Limnology and Oceanography*, *64*(2), 558–574. https://doi.org/10.1002/lno.11059

Zeng, X., & Beljaars, A. (2005). A prognostic scheme of sea surface skin temperature for modeling and data assimilation. *Geophysical Research Letters*, *32*, L14605. https://doi.org/10.1029/2005GL023030

Zeng, X., Zhao, M., & Dickinson, R. E. (1998). Intercomparison of bulk aerodynamic algorithms for the computation of sea surface fluxes using TOGA COARE and TAO data. *Journal of Climate*, *11*(10), 2628–2644. https://doi.org/10.1175/1520-0442(1998)011<2628:IOBAAF>2.0.CO;2

Zhang, R.-H., & Zebiak, S. E. (2002). Effect of penetrating momentum flux over the surface boundary/mixed layer in az-coordinate OGCM of the tropical Pacific. *Journal of Physical Oceanography*, *32*(12), 3616–3637. https://doi.org/10.1175/1520-0485(2002)032<3616:EOPMFO>2.0.CO;2

Zilitinkevich, S. S., Grachev, A. A., & Fairall, C. W. (2001). NOTES AND CORRESPONDECEScaling reasoning and field data on the sea surface roughness lengths for scalars. *Journal of the Atmospheric Sciences*, *58*(3), 320–325. https://doi.org/10.1175/1520-0469(2001)058<0320:NACRAF>2.0.CO;2